ROLE OF L1-FGFR INTERACTION IN GLIOMA PROGRESSION

by

Vishnu Mohanan

A thesis submitted to the Faculty of the University of Delaware in partial fulfillment of the requirements for the degree of Master of Science in Biological Sciences

Fall 2011

ROLE OF L1-FGFR INTERACTION IN GLIOMA PROGRESSION

by
Vishnu Mohanan

Approved: _____
Deni S. Galileo, Ph.D.
Professor in charge of thesis on behalf of the Advisory Committee

Approved: _____
Randall L. Duncan, Ph.D.
Chair of the Department of Department Name

Approved: _____
George H. Watson, Ph.D.
Dean of the College of College Name

Approved: _____
Charles G. Riordan, Ph.D.
Vice Provost for Graduate and Professional Education

ACKNOWLEDGMENTS

I would like to express my sincere gratitude to Dr. Deni S. Galileo for giving me this wonderful project. He has been the most extraordinary mentor I have ever had. His guidance and motivation made me an independent thinker. The techniques I have learned during the short frame are so valuable to pursue my goals in the future. Dr. Murali Temburni, without whom I would not have perfected the molecular cloning and various other methods. His presence in the lab during the weekends motivated me to work beyond the call of duty and to successfully complete the venture in the short time frame.

I would like to thank all my committee members, Dr. Donna Woulfe and Dr. Kenneth vanGolen, for their valuable comments, and supporting as well as criticizing the work at various stages of its progress. I would like to appreciate Karma Pace McDuffey, Michelle Pusey, Hamza Bhatti, Ryan Hartman, Grace Yang, Kalyani Chillukuri, Yupei Li and all my friends in UDel.

I would like to dedicate my work to my family back in India, without their encouragement I would not have been able to make it this far.

TABLE OF CONTENTS

LIST OF TABLES

LIST OF FIGURES

LIST OF ABBREVIATIONS

FGF	Fibroblast growth factor
FGFR	FGF Receptor
ADAM	A Disintegrin and Metalloproteinase
MMP	Matrix metalloproteinase
MAP	Mitogen-activated protein kinase
CAMs	Cell adhesion molecules
Ig	Immunoglobulin
FN	Fibronectin
NCAM-L1	Neural cell adhesion molecule-L1
GBM	Glioblastoma multiforme
BM	Brain metastasis
CNS	Central nervous system
FAK	Focal adhesion kinase
WT	Wild type
Tyr	Tyrosine
Src	Non-receptor tyrosine kinase related to sarcoma-causing v-src
Lvv	Lentiviral vector
ΔFGFR1	Truncated FGFR1 (kinase-deficient)
IRES	Internal ribosome entry site
MCS	Multiple cloning site

s.e.m	Standard error of the mean
GFP	Green fluorescent protein
RNA	Ribonucleic acid
mRNA	messenger RNA
shRNA	Short-hairpin RNA
DNA	Deoxyribonucleic acid
FACS	Fluorescent-activated cell sorting (flow cytometry)
L1LE	L1 Long Ectodomain
PCR	Polymerase chain reaction
DMEM	Dulbecco's Modified Eagle's Medium
P/S	Penicillin/Streptomycin
FBS	Fetal bovine serum
ATCC	American type culture collection
HEK	Human embryonic kidney
HRP	Horseradish peroxidase
HGF	Hepatocyte growth factor
RTK	Receptor tyrosine kinase
PDGFR	Platelet derived growth factor receptor
EGFR	Epidermal growth factor receptor
RGD	Arg-gly-asp amino acid
PNS	Peripheral nervous system
PBS	Phosphate buffered saline
TBS	Tris buffered saline

TBST	TBS + Tween 20 solution
mAb	Monoclonal antibody
CD171	Cluster of differentiation 171
PTA	Phosphotungstic acid
KDa	Kilodalton
BLAST	Basic local alignment search tool
CE	Cell extract
ECM	Extracellular matrix
CHD	CAM homology domain
TX-100	Triton X-100
CO2	Carbon dioxide
µg	Micrograms
µl	Microliter
ml	Milliliter
M	Molar
mM	Millimolar
nM	Nanomolar
$CaCl_2$	Calcium chloride
$MgCl_2$	Magnesium chloride
NaCl	Sodium chloride
BBS	BES-buffered saline
$CaPO_4$	Calcium phosphate
RIPA	RadioImmuno precipitation assay

SDS-PAGE	Sodium Dodecyl Sulfate--PolyAcrylamide Gel Electrophoresis
PVDF	PolyVinylidene Flouride
EDTA	Ethylenediaminetetraacetic acid
dNTP	Deoxyribonucleotide triphosphate
1xTAE	Tris acetate and EDTA

ABSTRACT

The L1CAM cell adhesion/recognition molecule (L1CAM, CD171) and Fibroblast Growth Factor Receptor (FGFR) are expressed by human high-grade glioma cells. L1CAM is a cell adhesion molecule that has homophilic interactions as well as heterophilic interactions with FGFR and integrins. Our lab previously showed that L1CAM cleavage is associated with an increased rate of migration of glioma cells and this correlates with increased focal adhesion kinase (FAK) activation. FGFR activation via its canonical FGF ligand leads to the transmission of intercellular signals responsible for cell proliferation, migration and survival. It has been observed that FGFR1 is expressed in glioma tissues, but is absent in the normal surrounding brain tissue. Analyzing datasets from a wide range of clinical samples showed that FGFR1 is over expressed in glioma samples regardless of its grade, while there is a gradual increase in the expression level of ADAM10 with the progression of glioma to various grades. In this study I used short hairpin RNA (shRNA) and dominant-negative approaches to inhibit the expression and activation of L1CAM and FGFR1, respectively. An L1-CHD peptide that inhibits L1-FGFR interaction and PD173074, a chemical inhibitor of FGFR1, also were used to elucidate the involvement of L1-FGFR interactions on glioma cell behavior. Migration studies and cell cycle analyses showed the relevance in the contribution of L1CAM towards FGFR activation. Also. L1CAM interaction with FGFR had no effect on cell proliferation on subconfluent cultures, while blocking L1-FGFR on confluent glioma cell decreased the S phase to

43% compared to the untreated. It was also observed that L1CAM attenuated cells exhibited almost the same amount of reduction in migration as in cells deprived of FGFR signaling. While specifically blocking L1-FGFR interaction there was a decrease of 50% in migration rate in T98G cells compared to the control cells, and there was a decrease in 24% in U-118/L1LE cells compared to the control cells. This study showed that treatment of glioma cells through FGFR inactivation by targeting only its native FGF ligand might be ineffective due to a major contribution of the receptor activation through L1CAM. Both L1CAM and FGFR1 shutdown glioma cells exhibited a complete termination of cell migration *in vitro*. These results indicate that L1CAM modulates motility and proliferation of human glioma cells via signaling through the FGFR. This could justify the relevance of targeting a cell adhesion molecule as well as a robust receptor in the treatment of malignant gliomas by disrupting cell invasion and growth.

Chapter 1

INTRODUCTION

The central nervous system (CNS) is considered one of the chief systems having the least regenerative capacity in humans. Neuronal cells lose their migratory tendency as they mature. A cancerous tumor that arises in the brain, overcoming its normal cells' migratory and reproductive "dormant" stage, is one of the common cancers evading all current treatments. Could a therapy be imposed without compensating for both cell division and invasion of the cells into normal brain tissue? Would there not be more than one 'queen' molecule to be targeted in order to destroy the tumor 'hive'? Surgery remains the primary treatment, but because some cells have already migrated into brain parenchyma they escape resection.

There is no evidence for gene amplification of the fibroblast growth factor receptor (FGFR) associated with glioblastoma, the highest grade of glioma brain cancer. But alternatively, in order to increase the activity of a receptor, rather than increasing its production, an increase in ligand expression could saturate the receptors, enhancing its activation level. ADAM10 protease up regulation resulting in an increase in cleavage of the transmembrane protein L1CAM[1], a cell adhesion molecule having an affinity towards FGFR and Integrins, would result in a recurrent activation of its receptors.

The variety of roles, including cell migration, performed by cell adhesion molecules[2] clearly elucidates its importance in glioma progression, where there is an up regulation in cleavage of L1CAM – releasing fragments into the ECM – making

the cells less adhesive and trigger the cellular signaling for migration. For cells to migrate there should be an optimal level of adhesion towards the ECM, axons or any other body through which they migrate. Normal glial cells expressing L1CAM have a strong attachment with the body onto which it is adhered. Cancerous cells release L1CAM, making them less adhesive, but the presence of other cell adhesion molecules expressed on the cell membrane will give the cells the appropriate grip to migrate.

Here, I elucidate how the **neural recognition molecule L1CAM (L1)** stimulates the motility and invasiveness of GBM cells by signaling through the **fibroblast growth factor receptor (FGFR).** Elucidating mechanisms of glioma cell dispersal and devising strategies to block them should improve patient survival by allowing for more complete surgical resection.

1.1 Glioma

Glioblastoma multiforme (GBM), one of the most common type of adult brain cancers [1][2] [3] till date has no successful treatment. It comprises 2% of all diagnosed cancer, with a median survival time between 9 and 12 months. It is the most frequent neuroepithelial malignancy, with an adjusted incidence rate of 2.6 new cases per 100,000 people. Seventy percent of Glioblastoma has its origin in the frontal and temporal lobes and twenty percent in the parietal lobe of the brain [4]. Pathological characteristics of GBM include hypercellular structure, necrotic foci with peripheral cellular pseudopalisading (represented by arrow in Fig. 1), hypermicrovascular formation, and hyperchromatism. Glioma can be classified into astrocytoma, ependymoma and oligodendroglioma, among which astrocytoma are the most

common type. The cellular origin of these tumors still remains unknown, although there is evidence that brain stem cells or potentially proliferating related cells are able to change into tumor stem cells, which form the malignant gliomas.

Table 1 WHO grading of astrocytoma (Stiles and Rowitch)

	Pilocytic Astrocytoma (WHO grade I)	Diffuse Astrocytoma (WHO grade II)	Anaplastic Astrocytoma (WHO grade III)	Glioblastoma a.k.a. Glioblastoma Multiforme (WHO grade IV)
Age of Onset	First two decades of life	30 to 40 yrs	Early 40s	Mid 50–60s
Typical Location	Throughout the neuraxis. Optic pathway tumors are frequent	Cerebral hemispheres. Pons/brainstem, esp. in children	Cerebral hemispheres	Cerebral hemispheres
Average Survival	Years to decades	Five years	Two to five years	Fourteen months

Surgery remains the primary treatment for GBM, but because cells tend to migrate into brain parenchyma they escape resection. Adjuvant drug and radiation treatment kills most remaining cells, but resistant glioma tumor-initiating or "stem" cells reinitiate tumor growth [5][6][7][8][9]. Treatment strategies that target migrating GBM cells are critically needed [10], but mechanisms that control GBM cell dispersal and behavior such as perineuronal satellitosis [11] are not known. GBM has a five-

year survival rate of an average of <4%, which has not improved in the past 30 years [12].

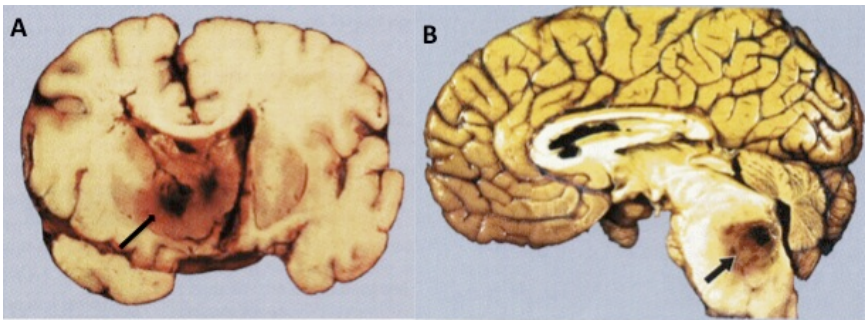

Figure 1 **GBM anatomy. A) coronal section through the parietal-occipital junction. Arrow represents the recent hemorrhage, necrosis and areas of firm tissue. B) A midsagittal view of a human brain where glioma is represented in arrow in the dorsal pons. [A. D'Agostino, Good Samaritan Hospital, Portland, Orgeon.**

1.2 L1CAM

1.2.1 Structure and function of L1CAM

L1CAM (L1) is a type I transmembrane glycoprotein of about 200-220 kDa molecular weight belonging to the immunoglobulin super family. Its extracellular region consists of six immunoglobulin- like domains (Ig) and five fibronectin-like repeats (FN) (fig. 2). The relatively short intracellular cytoplasmic domain consisting of 120 amino acids binds to some proteins and in turn transmits a series of physiological effects [13]. The long extracellular region facilitates the molecule to be modified by glycosylation, and in turn allows it to participate in various cell-cell interactions. It is the founder member of the L1 subfamily of Ig cell adhesion molecules (IgCAMs) expressed in the nervous system. It is highly conserved in mammals with 80-90% amino acid in each of the extracellular regions, and 100% identity in the cytoplasmic domain in humans, rats, and mice [14]. Cell–cell adhesion

facilitated by this molecule is mediated through Ca2+-, Mg2+-independent homo- or heterophilic binding at the cell surface [15][16].

The neuronal isoform of L1CAM is a full length protein expressed on the surface of neurons, especially axon growth cones. It is formed by alternative splicing to contain a 12-nucleotide exon-27 encoding the amino acid sequence (RSLE) inserted into the cytoplasmic domain to help in recruiting the AP2-clatherin adaptor for endocytosis [17]. It plays a crucial role in the developing CNS, facilitating neural migration, neuronal survival, as well as axon outgrowth, guidance, fasciculation, regeneration and synaptic plasticity in brain development and neural regeneration after trauma [18][19][20]. The non-neuronal isoform lacks exon-2 at the protein's N-terminus (define) and exon-27 within the intracellular region. It is normally found in Schwann cells in the peripheral system, some lymphocytes, and part of the renal system.

L1 is found on axon surfaces facilitating contact between axons on differentiated neurons. L1CAM extracellular region can be cleaved at two different sites and the released form of L1 gets embedded in the extracellular matrix and participates in cell-matrix interactions. The cleaved products would include a 180-200 kDa ectodomain and a 30 kDa transmembrane fragment, which would be further degraded by γ-secretase. Cleavage that occurs with the third FNIII domain by plasmin generates a 140 kDa fragment and a transmembrane 80 kDa fragment, which gets further cleaved to a 30 kDa transmembrane fragment. Membrane proximal L1CAM cleavage is mediated by ADAM10 (a disintegrin and metalloprotease) and is non-specific.

The significance of L1CAM in human development comes under the spotlight with severe brain malformations resulting from various L1 gene mutations, which is categorized as L1-syndrome [17][18][22]. Several recessive neurological diseases including MASA (Mental retardation, Aphasia, Shuffling gait, and Adducted thumbs) syndrome [22], SP1 (spastic paraparesis type 1), ACC (X-linked agenesis of corpus callosum) and other X-linked neuronal diseases [23] are now grouped into the larger category of L1 syndrome. One of the most severe symptoms of L1 syndrome is hydrocephalus, which is caused by mutations leading to premature extracellular L1 truncation and secretion [17][22].

L1CAM contributes to the progression of human tumors, but the mechanism is still not clear. Several recent studies show that overexpression of L1CAM triggers cell motility and invasion of carcinoma cells on extracellular matrix proteins and matrigel respectively [24][25][26][27][28].

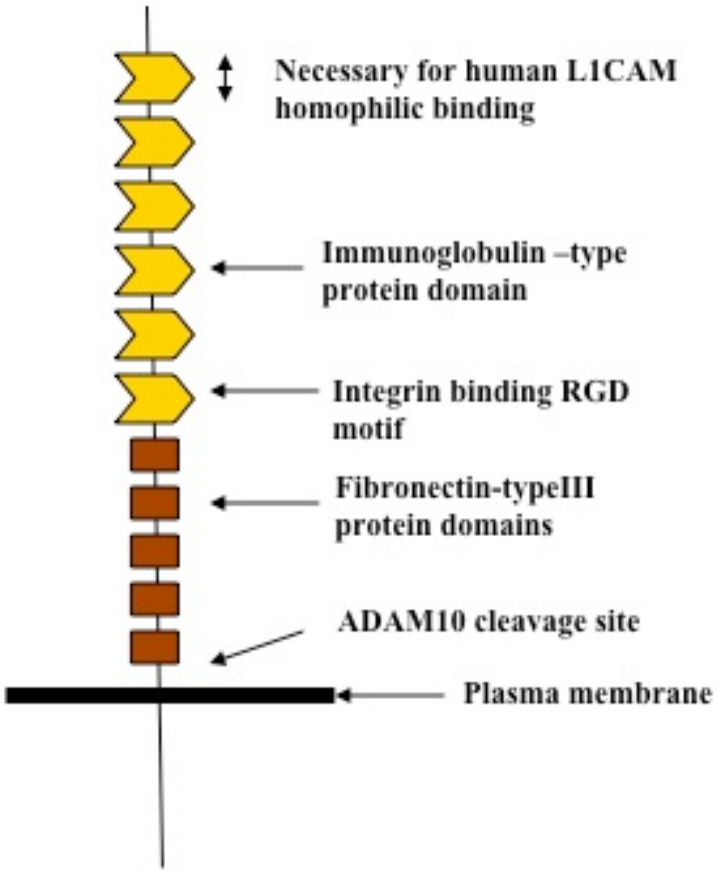

Figure 2 **L1CAM Schematic.** L1CAM is a type-one transmembrane glycoprotein. It has 6 Ig domains, 5 Type III fibronectin-like repeats, a transmembrane region and a highly conserved cytoplasmic tail. The diagram is generated by Vishnu M.

1.2.2 Binding partners of L1CAM

L1CAM mediates homophilic interactions as well as interactions with other molecules such as FGFR, other Ig-domain CAMs (such as NCAM, TAG-1/axonin-1, and F11/contactin), two proteoglycan-type molecules (neurocan and phosphacan), RGD-specific integrins $\alpha_5\beta_1$ and $\alpha_V\beta_3$), and extracellular matrix molecules (including laminin and certain tenascin forms). It also binds to DM-GRASP (another IgCAM) to promote neurite outgrowth [29]. My work is based on its interaction with the FGFR. As mentioned before, L1CAM itself can transmit a signal through its cytoplasmic domain, with its interaction with proteins such as cytoskeletal elements, protein kinases and a celluar protein complex that is involved in endocytosis and intracellular protein trafficking [30]. The cleaved L1CAM fragment in the intracellular region has been reported to be transported to the nucleus where it could act as transcriptional factor [117]. L1 interactions in *cis* are essential to promote neurite outgrowth [31]. L1CAM interaction with other molecules can be classified in three different modes such as: 1) membrane bound L1 interaction, 2) cleaved L1 ectodomain sequence having an autocrine and paracrine effect, and 3) exosome vesicles decorated with L1CAM released from the cells.

It is believed that cell membrane protein cannot transmit signals intracellularly unless these molecules gets bound to another molecule. Evidences suggest that L1CAM forms dimers or multi-protein dimer complexes in the membrane of a growth cone. L1 binding partners include FGFR, glycosylphosphatidylinositol (GPI)-anchored CAMs (TAG-1/axonin-1 or F3/F11/contactin), DM-GRASP, and L1

itself. Work published by the Doherty and Walsh group indicated the interaction of L1 and FGFR and its involvement in neurite outgrowth. L1's interaction with nonreceptor tyrosine kinase pp60c-src and L1 cis-heterodimerization with TAG-1/axonin-1 is also required for L1 mediated neurite outgrowth. Most of the homo and heterodimerization patterns have not been directly demonstrated but this idea shows that dimerization is common for members of the Ig superfamily in the immune system [32]. Inhibition of FAK, Ras, Raf and MEK impairs NCAM- and L1CAM-dependent neurite growth, which shows the involvement of L1CAM towards the MAP kinase signaling pathway [33].

L1 can interact with various integrin receptors stimulating cell growth [24]. Evidence from my lab showed the co-localization of L1 with FAK (Focal Adhesion Kinase) [118], however, L1 also bound to areas of glioma cell surfaces separate from those of FAK activation. L1 interaction with integrins triggers FAK activation thereby altering the focal adhesion complex turnover [60].

1.3 FGF Receptor

The FGFR is a tyrosine kinase receptor with various isoforms, having extracellular immunoglobulin domains and an intracellular tyrosine kinase domain.(Fig. 3) Fibroblast growth factors (FGFs) are its canonical ligands [35].

1.3.1 Structure and Function of FGFR

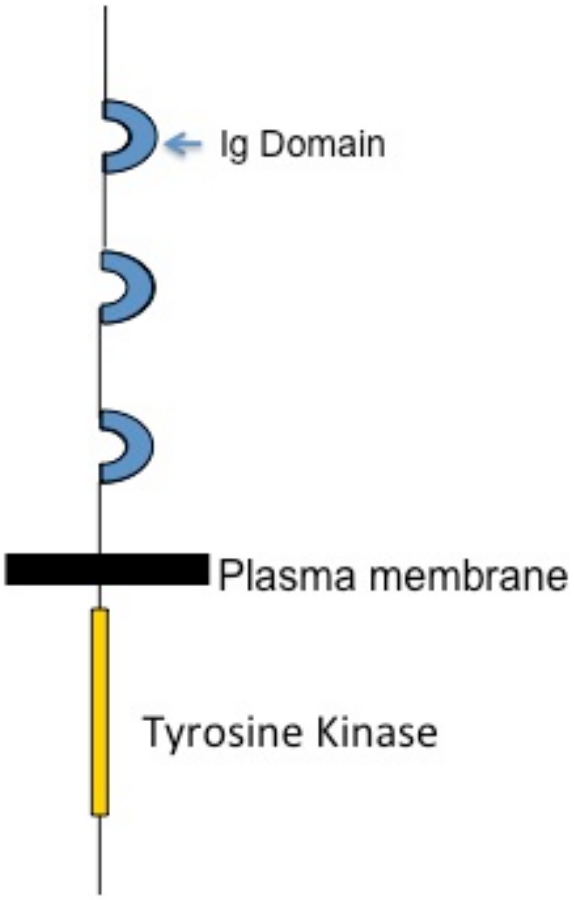

Figure 3 **FGFR Schematic.** Fibroblast Growth Factor Receptor is comprised of 3 extracellular immunoglobulin domains and a highly conserved intercellular kinase domain. The image is generated by Vishnu M.

Encoded by four genes (FGFR 1-4), FGFRs exist in seven principle variants generated by alternative splicing in the extracellular Ig-like domain adjacent to the membrane. FGFR isoforms differ in their binding affinity towards the FGF ligands. Studies have demonstrated a significant redundancy in FGF-FGFR interactions with all major FGFR variants being activated by at least five FGF ligands, but this redundancy appears limited *in vivo* [34]. Heparan sulfate is a critical component in FGF signaling *in vivo* and *in vitro* through a strong interaction with FGF and facilitating an active interaction with FGFR [35]. There are seven tyrosine residues (Tyr463, Tyr583, Tyr585, Tyr653, Tyr654, Tyr730, and Tyr766) in the cytoplasmic domain of FGFR1, which serve as the substrate for phosphorylation. Tyr653 and Tyr654 directly contribute towards catalytic activity and signaling. Tyr766 binds the SH2 domain of PLC ϒ. Activity of the remaining residues is not known.

FGFR1 is predominantly expressed on neurons while FGFR2 and FGFR3 are primarily on glial cells [37]. FGFR4 is mainly responsible during the early development and is not detectable in the adult CNS [36][37]. The individual FGFRs have unique expression patterns *in vivo*, and affect cell behavior differently in both *in vitro* and *in vivo* experimental models [38][39][40]. Studies comparing the signaling capacity among the individual FGFRs however show that they activate their downstream signaling in a similar fashion, with the major differences being quantitative [41][42]. The signaling specificity of individual FGFR type is further complicated by the fact that most cells express more than one FGFR variant and FGFRs can form active heterodimers [43].

FGFR signaling regulates fundamental development pathways that control events such as mesoderm patterning in early embryo to the development of multiple organ systems [44][45]. It also has physiological roles in the adult organism, which include regulation of angiogenesis and wound repair. The FGF family serve as important signals in the developing , adult and lesioned nervous system. FGFR knockout mice have been extensively used to study the significance of the receptor. They are expressed by a variety of tissues and regulate cell differentiation, proliferation and survival and this makes the receptor susceptible to be contributor for tumorogenesis.

1.3.2 FGFR ligands and signaling

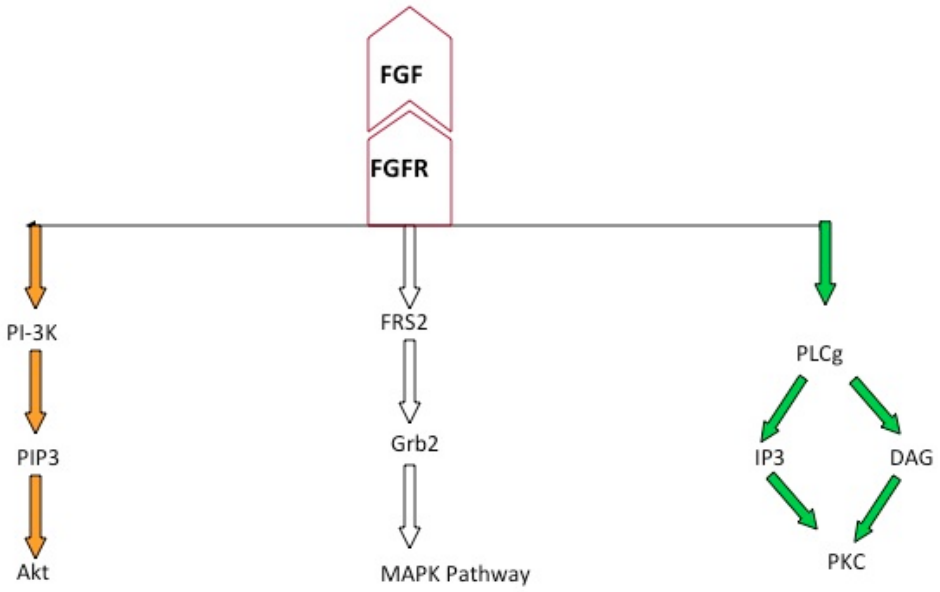

Figure 4 **FGFR signaling pathways.** FGF Receptor activated by its FGF ligand can elicit various intercellular signaling pathways responsible for cell proliferation, migration and survival.

FGFRs have affinity towards a variety of molecules such as FGF (22 isoforms), L1CAM, N-cadherin, NCAM, and EphA [46]. The interaction with L1CAM is explained in detail below. EphA is another transmembrane tyrosine kinase protein containing an external Cys-rich domain and 2 fibronectin type III repeats, which have been implicated in mediating developmental events, particularly in the nervous system. N-cadherin belongs to Type I transmembrane proteins which are involved in cell adhesion (Calcium-dependent) in neurons. The synergistic activity of FGFR and N-cadherin was shown to generate intracellular signals that promote neuronal growth [46][47].

As shown in figure, the receptor activation leads to activation of signaling pathways responsible for cell proliferation, differentiation, migration and survival. The Tyrosine Kinase receptor undergoes dimerization when it interacts with its ligands. Further, through cross-phosphorylation the tyrosine residues in the cytoplasmic domain become activated. FGFR employs several signaling pathways in their downstream intracellular signaling, including ERK and p38 mitogen activated kinases, and phospholipase-C-gamma (PLCγ). With the exception of PLCγ that binds directly on the phosphorylated Y766 of the activated FGFR, FGFRs recruit their downstream signaling via phosphorylation of several signaling adaptors such as Gab1, SHB. SHC and FRS2. FRS2 plays a major role for FGFR mediated activation of ERK and P13K pathways [48]. Crk, an SH2/SH3-containing adaptor protein is also suspected to link FGFR with Shc, C3G, and Cas during the intercellular signaling. Tyrosine-phosphorylation-independent signaling by FGFRs also takes place which involves a 90 kDa phosphoprotein, SNT-1, or FRS2. It transmits signals to the Ras/MAPK signaling pathway. This is by recruiting Ras to FGFR complex through

the adaptor protein Grb-2/SoS. FRS2 can also bind protein tyrosine phosphatase Sh2. [49][50].

In summary, FGFRs mediate signal transduction in two independent pathways. Firstly, it utilizes an SH2-linked pathway to link FGFR with PLCγ and Crk. Secondly, it links to SNT1/FRS2 through an interaction at the juxtamembrane domain.

1.4 L1-FGFR interaction

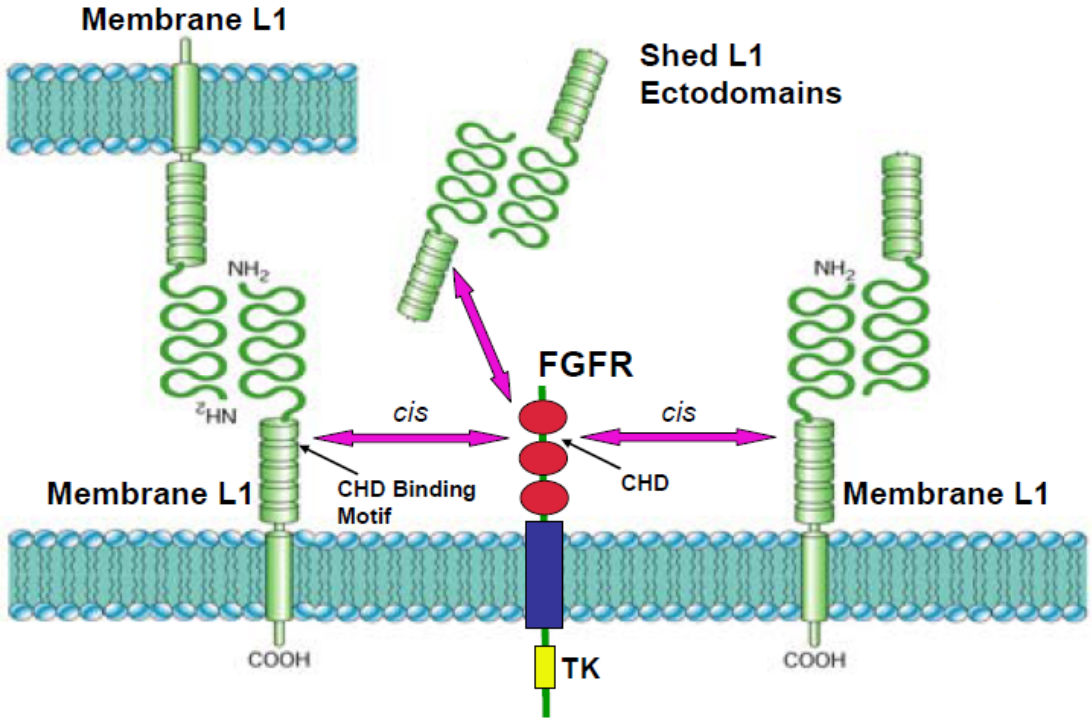

Figure 5 **L1–FGFR potential interaction model.** FGFR binds with L1CAM which is either bound to cell surface or the proteolyzed L1 ectodomain. Only one FGFR is shown for simplicity. The diagram was provided by Galileo D.S.

Sequence alignment of individual L1CAM FN3 modules with various FGFs suggested that four sequence motifs located in the third and fifth L1 FN3 modules might be involved in interactions with FGFR [51]. The structure of the FN3 module 2 was determined by nuclear magnetic resonance(NMR) analysis, and it was shown to interact with the FGFR Ig module 3[52]. Using Surface Plasmon Resonance (SPR) analysis it was shown that NCAM FN3 modules 1 and 2 bind to FGFR Ig modules 2 and 3 with a 10 _M Kd, a value significant enough for an efficient binding between NCAM and FGFR under physiological conditions, which was confirmed by co-immunoprecipitation of NCAM with FGFR [52]. Immunobot assay using antibodies against phosphorylated tyrosine in FGFR, stimulated by FN3, proves its ability to activate the receptor [53].

The CAM- homology domain (CHD) in the FGFR, which resides between Ig-like domains 1 and 2, interacts with the putative FGFR-CHD binding motif in the FNIII domain 4 of L1. This activates the tyrosine kinase domain of the FGFR and subsequent activation of phospholipase Cg (PLCg). PLCg then hydrolyzes phosphatidylinositol to generate inositol phosphate and diacyl- glycerol (DAG). DAG lipase converts DAG to arachidonic acid which increases Ca^{2+} influx through N- and L-type Ca^{2+} channels, and the local increase in Ca^{2+} levels activates Ca^{2+}/calmodulin kinase II and probably other kinases [54].

1.5 Dominant negative approach to shutdown receptor signaling

A dominant negative approach has been successfully employed to shut down the activation of molecules especially for Tyrosine Kinase Receptors. Over-expression of a truncated gene, devoid of the intercellular region, would prevent the

cross phosphorylation during the process of ligand-activated receptor dimerization. This process would permanently stop the cells, expressing the truncated molecule, to respond to signals transferred through this receptor [55]. This approach is used successfully to inhibit FGFR activation in several cell types. It has been shown that 10-75 fold excess in truncated FGFR1 inhibits all wild-type responses. It can also inhibit the signal transduction via FGFR2 and FGFR3 as well due to heterodimerization [55] [56]. Truncated FGFR1 expressing oligodendrocyte progenitors were unable to migrate when transplanted into neonatal rat brains [93].

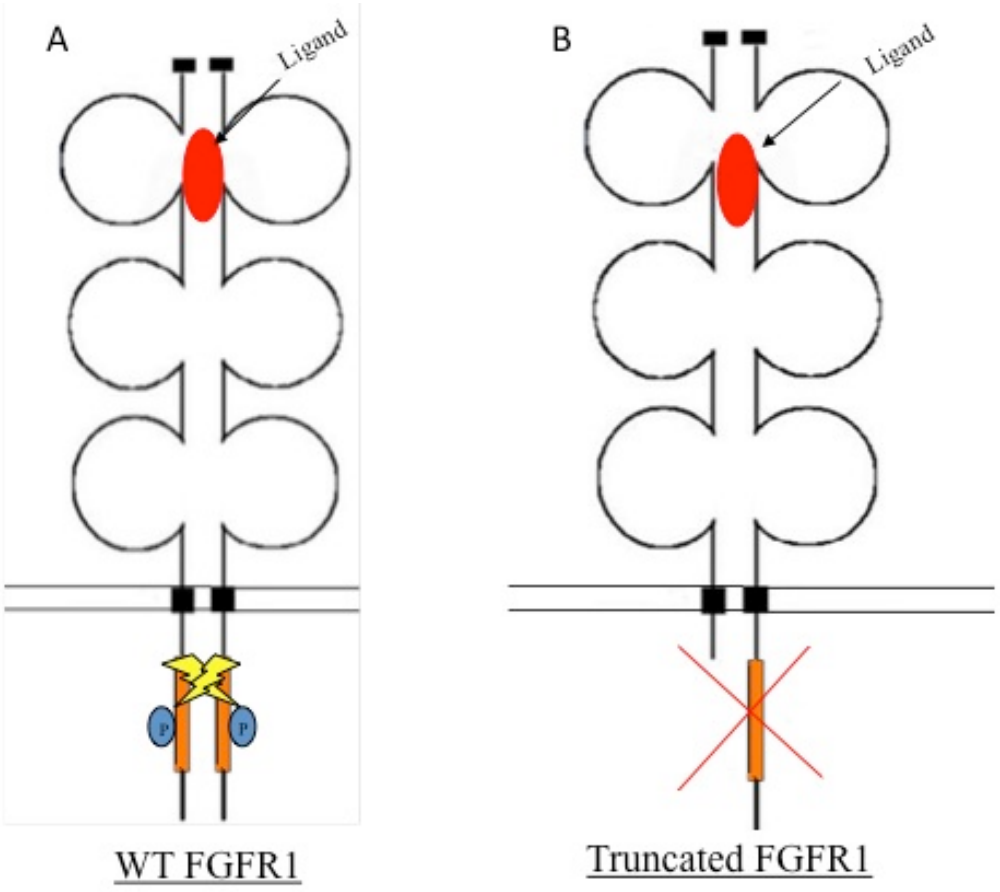

Figure 6 **Schematic diagram of Dominant-Negative FGFR1 mechanism.** A) Wild type FGFR1 activation. Ligand binding results in receptor dimerization, which results in cross-phosphorylation of tyrosine residues in the cytoplasmic domain of the receptor. B) Expression of a truncated FGFR1 sequence devoid of tyrosine residues competes with the native receptors during ligand-activated dimerization, which leads to lack of cross-phosphorylation.

1.6 L1CAM in invasive cancer

L1CAM has been attributed with the progression of different types of cancer. L1CAM triggers a constant activation of β-catenin TF signaling, which is one the major pathways that modulates colon cancer progression [57]. In ovarian cancer, L1CAM expression was detected in 79% of human samples and also correlates with poor prognosis and metastasis [58]. L1CAM also has been identified as a novel marker in carcinoma progression [59]. In renal cell carcinoma, L1CAM is expressed in tumor tissue originating from cells that do not express L1CAM and it also correlates with metastasis. Gene array analysis from malignant tissue detected a higher level of L1CAM RNA compared with the non-malignant nervous tissue [119]. L1CAM expression is much more common in poorly differentiated tumors as compared to with the differentiated tumors [57]. My lab findings have shown that shutting down L1 in glioma cell lines slows down motility (migration velocity) on culture dishes and impeded invasion in brain [60][87]. L1CAM expression is also correlated with breast cancer progression [61][120].

The mechanism involving L1CAM contributing towards tumorogenesis is through activating MAP kinase, AKT pathway and extracellular-signal-regulated kinase (ERK) as shown in fig. 7. This is through interaction and activating receptor tyrosine kinase such as FGFR, EGFR (epidermal growth factor receptor), hepatocyte growth factor receptor (HGFR), integrins and several other receptors as described before. The ectodomain released mediated by the cleavage through MMPs will have an autocrine and paracrine effect in stimulating cells. Also it has been shown that exosomal vesicles having L1CAM on its surface accelerates the process [121].

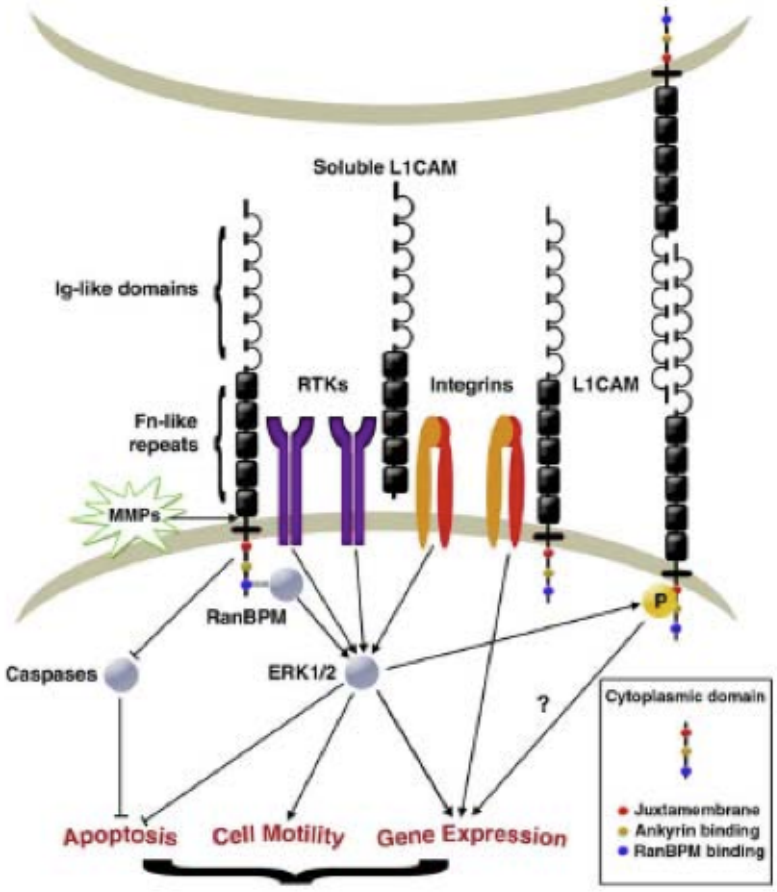

Figure 7 **L1-receptor interaction and signaling pathways.** As a cell adhesion molecule, L1CAM participates in different cell interactions homophilically or heterophilically in tumors. Surface or cleaved L1 by ADAMs can *cis*-interact with membrane RTKs and integrins, leading to ERK activation. The cytoplasmic tail of L1 can be phosphorylated, or binds to different adaptor proteins as RanBPM or ankyrin in the cytoplasm to initiate signaling transduction. Through various pathways, L1CAM promotes cell motility and proliferation but inhibits apoptosis, all contributing to tumorigenesis. [adapted from 92].

1.7 Contribution of FGFR in glioma and different types of cancer

Receptor tyrosine kinase genomic alteration has been implicated in GBM growth. One of the receptors that is investigated as a therapeutic target includes Epidermal Growth Factor Receptor (EGFR). It also has been identified in glioblastoma that there is a low level incidence of point mutations in FGFR1 tyrosine kinase domain but there is no evidence for genomic amplification at the FGFR1 loci [62]. It has been shown that expression of FGFR1 is up-regulated in GBM compared with normal white matter. FGFR inactivation has been implicated with a decrease in glioma proliferation [99][100][63]. It has been observed in FGFR1 knock out mice that the tumor mass was significantly reduced and also impaired of angiogenesis [64][65][66]. My work would bring into highlight one of the ligands responsible for this proactive receptors activity and the contribution of FGFR in GBM motility *in vitro*.

It has been recently found that Src kinase regulates activation and signaling dynamics of FGF receptors [67]. As shown in figure 8, the FGF Receptor signaling is largely tumor specific, where it can be genomic alterations that drive ligand-independent receptor signaling or activation through a ligand-dependent manner. Genetic alterations have been attributed to the progression of several maliganancies. FGFR1 gene amplification, mutation and translocation is observed among breast cancer, melanoma and stem cell leukemia respectively [68][69][70][71][72][73][74][75]. Gastric cancer, endometrial cancer, salivary adenoid cystic cancer, bladder cancer, myeloma, colon and lung adenocarcinoma are some other tumors which are associated with FGFR gene alterations [76][77][78][79][80][81][82].

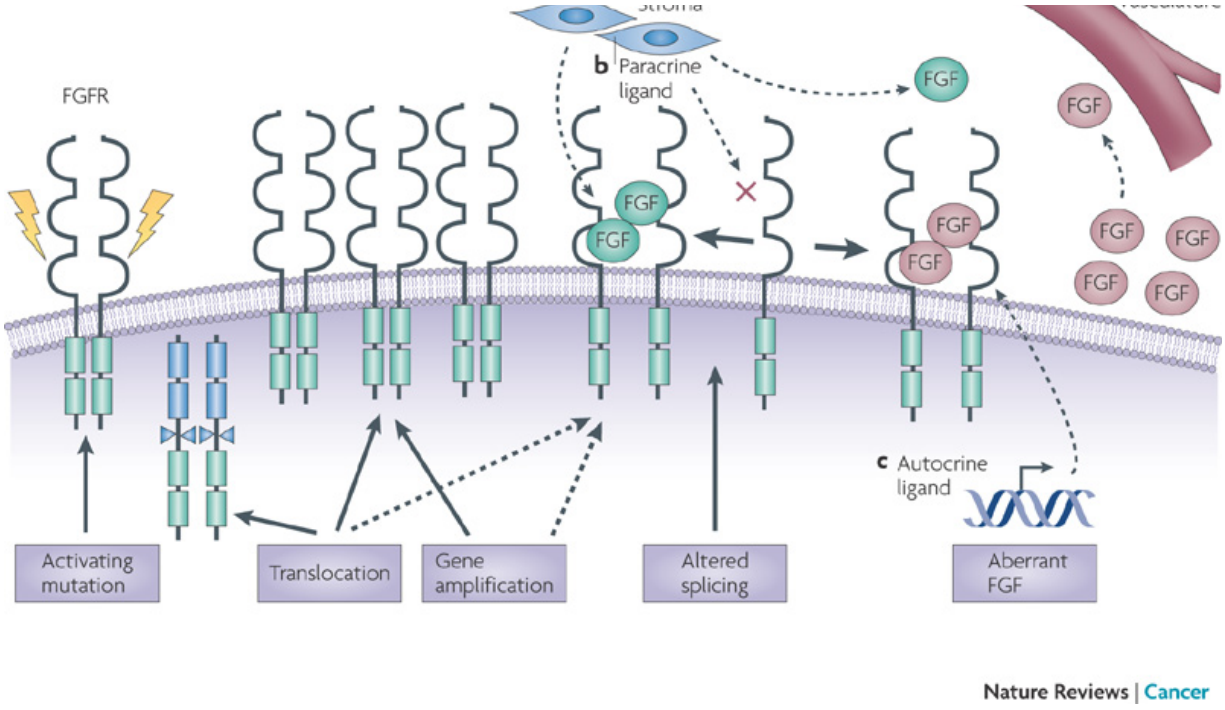

Figure 8 **Mechanisms of cancer cell signaling through FGFR.** FGFR signaling can contribute towards cancer progression either through direct receptor manipulation or through changes in its ligands either in its expression pattern or activation. **[117]**

1.8 Hypothesis and specific aims

Glioma motility and proliferation are enhanced by the autocrine effects of proteolyzed L1 interacting with FGFR1

- Aim 1: **To construct a lentiviral vector for truncated FGFR1 (ΔFGFR1) and to make stably infected glioma cells**

- Aim 2: **To determine the effect of blocking FGFR activity on glioma cell proliferation and migration.**

- Aim 3: **To determine the contribution of L1CAM-FGFR interaction on glioma cell behavior**

Chapter 2

MATERIALS AND METHODS

2.1 Cell lines and culture.

Human glioma cell lines used in this study were obtained from the American Type Culture Collection (ATCC, Manassas, VA). T98G is a human GBM cell line [115]. U-118 MG is a human Grade III astrocytoma cell line [116]. HEK293T/17 is a human embryonic kidney cell line. All the cell lines were cultured in DMEM, 10% FBS, 2 mM L-glutamine, and penicillin–streptomycin and incubated in a humidified incubator with 37^{O}C and 5% CO_2.

2.2 Antibodies and reagents

UJ127 (cat. # GTX72362; Gene Tex, Irvine, CA) is a mouse monoclonal antibody against the human L1CAM, which recognizes the 5th fibronectin repeat within the ectodomain. A concentration of 0.8μg/2ml was used for western blot analysis. HRP-conjugated goat anti-mouse (Jackson Immunoresearch) with a concentration of 0.4μg/3ml was used as the secondary antibody.

Monoclonal mouse anti-FGFR (cat. # 13-3100; Invitrogen) binds strongly to human and chicken FGFR1. A concentration of 4μg/2ml was used during western blot analysis. HRP-conjugated goat anti-mouse (Jackson Immunoresearch) with a concentration of 0.4μ/4ml was used as the secondary antibody.

A peptide sequence from the CAM homology domain (CHD) of FGFR1 was used to block L1-FGFR interaction [46]. NRMPVAPYWT is the peptide derived

from the CHD specific for L1. A scrambled peptide, VYMWRPTNPA, was used as control peptide (Genscript). The peptides were used at a concentration of 500µg/ml dissolved in 0.5% FBS supplemented DMEM media.

PD173074 (CAS # 219580-11-7; Sellek, Houston, TX) is an FGFR1 inhibitor. PD173074 specifically blocks the phosphorylation of FGFR1with an half maximal inhibitory concentration (IC50) value of 21.5nM [83][84] and it weakly inhibits PDGFR and c-Src with an IC50 of 17.6 and 19.8µM, respectively).

Restriction enzyme BamH1 (cat # R0136S New England Biolabs) and Xho1 (cat # R0146S) were used during the Lentiviral vector construction. T4 DNA ligase (cat # M0202S New England Biolabs) was used at concentration of .1µl per reaction mixture of 10 µl.

2.3 Lentiviral vector construction.

ΔFGFR1 sequence was obtained through PCR from the plasmid [(PNAS 86:5449), GenBank M24637] that carries the chicken FGFR1 isoform (CEK1). The cek1 cDNA in pBluescript SK+ plasmid was provided by Dr. Elena Pasquale (Burnham Institute). The primers used are:

Forward primer:

5’ CGCCGCGGATCCATGTTTACCTGGAGGTGC 3’

Reverse primer

5’ CCGCCGCTCGAGCAGCCTGTCCCGTGG 3’

The primers are encoded with restriction sites BamH1 and Xho1 at the 5’ end of the forward and the reverse primer respectively. The amplified product was run

on 1% agarose gel and the required band was gel purified. This constitutes the insert, when the sequence was double digested with BamH1 and Xho1.

Lentiviral vector (LVV) 2605 was obtained from Dr. John Kappes (Univ. of Alabama, Birmingham). The MCS (Multiple Cloning Site has the sequences for BamHI, SpeI, BclI, NheI, MluI, XbaI, and XhoI. The vector has puromycin selection marker expressed from an internal ribosomal entry site (IRES). It also has the sequence for GFP. Double digestion using BamH1 and Xho1 was performed on the vector to create cohesive compatible ends.

Ligation of the insert and the LVV was carried out at room temperature overnight using T4 DNA ligase. The ligated samples were transformed into chemically competent HB101 bacteria. Colonies were picked from LB-Amp plates and grown overnight. The plasmid was isolated from the bacteria using a plasmid mini prep kit. Miniprep DNA was double digested and run on a gel to determine insert size. Also the construct was run on PCR with the primers for ΔFGFR1 and the confirmed from DNA electrophoresis. Finally it was confirmed by DNA sequencing (GENEWIZ, Inc. South Plainfield, NJ). The gene product of this truncated form of FGFR will have only 483 amino acids in contrast to the 819 amino acids I its native form. (Figure). The Empty LVV 2605 acts as negative control.

The 1879 LVV carrying L1LE (L1CAM long ectodomain) sequence created by other Master's thesis students in the Galileo lab [120] was also used for the study. shRNAs (Lenti Virus) targeting human L1CAM, TRCN0000063917 (cat No. RHS3979-97052304) and the non-target shRNA control in the vector pLKO.1 were obtained from the company Open Biosystems (Huntsville, AL).

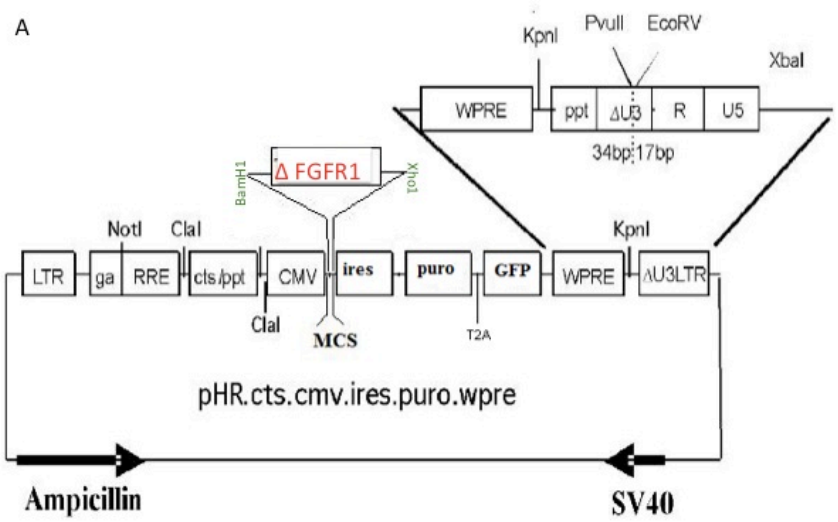

Figure 9 **Schematic diagram of LVV 2605 vector containing ΔFGFR1.** The vector contains puromyine resistant gene and GFP which are connected via T2A sequence. CMV promoter facilitates constant expression.

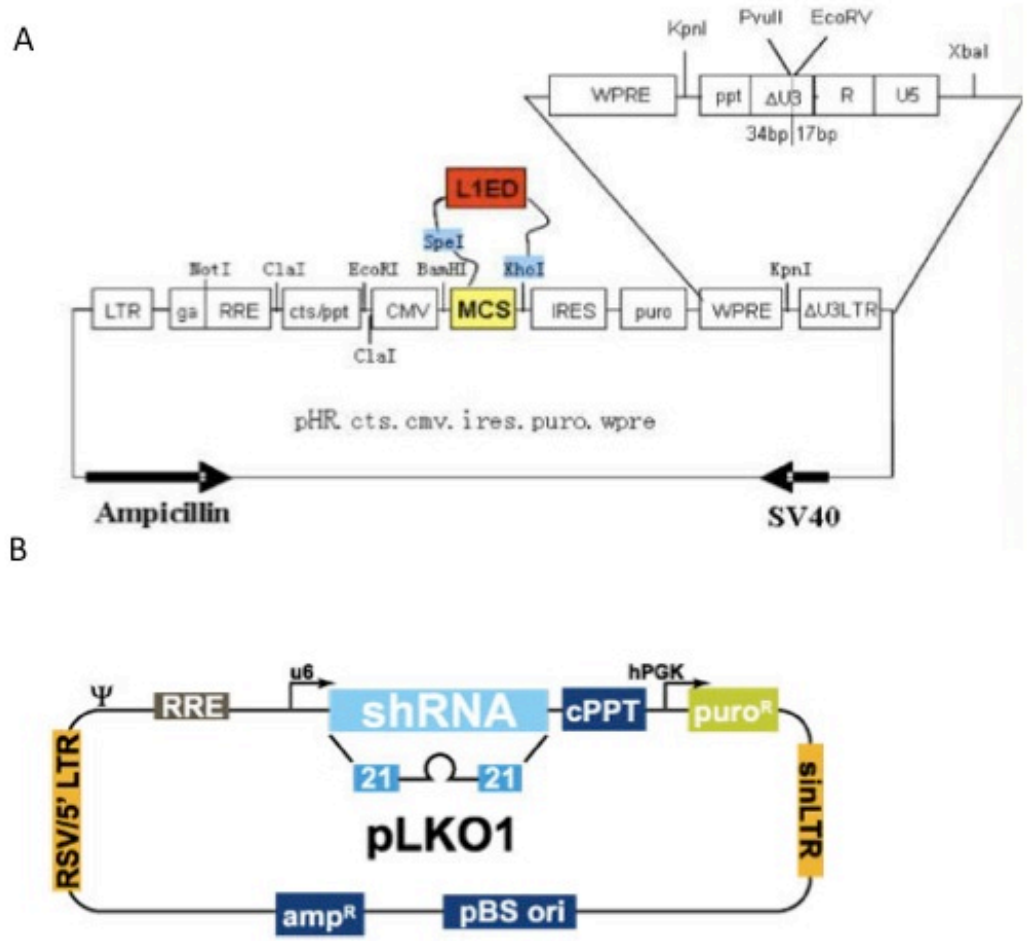

Figure 10 **Schematic diagram of LVV constructs A) Lentiviral vector L1LE (L1, 2010). B) Lentiviral vector pLKO.1 with L1shRNA from Open Biosystems.** The viral vectors were transfected in HEK cells along with the packaging plasmids and envelop plasmids in order to generate the virus.

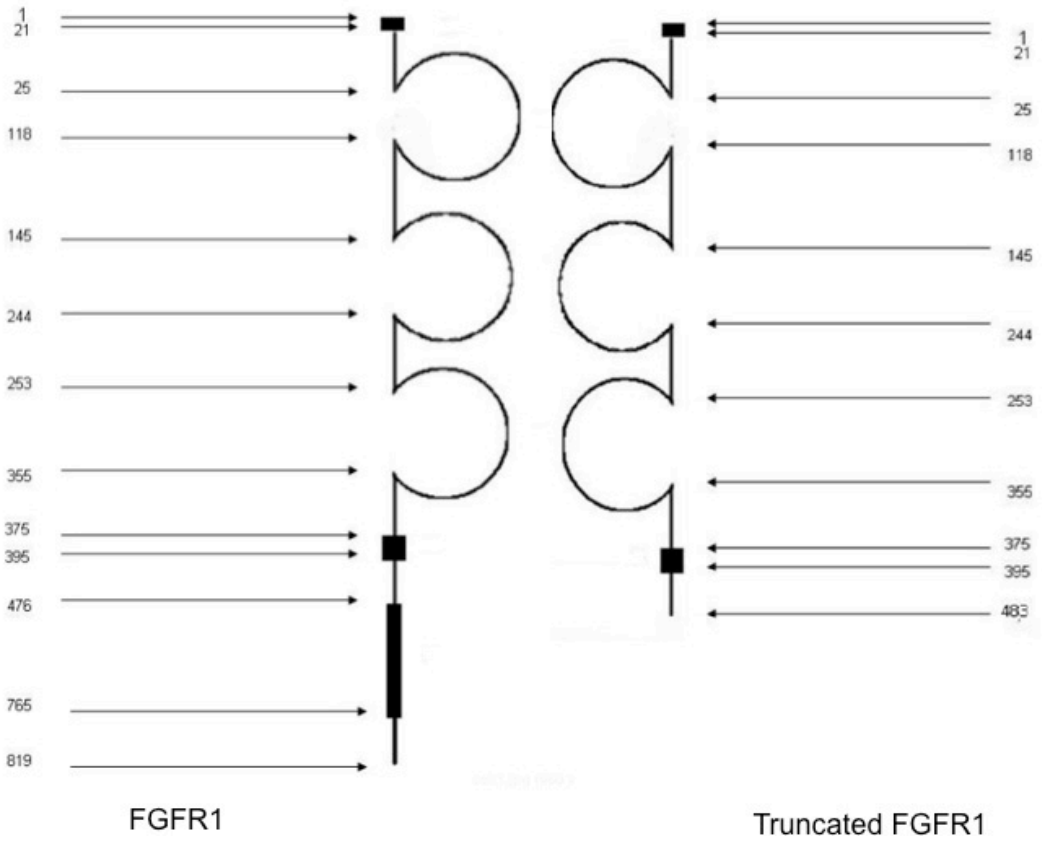

Figure 11 **Native and truncated FGFR1.** The native protein has 819 amino acids while he truncated will have only 483 amino acids.

2.4 Transfection and infection

HEK 293T cells were grown to a confluency of about 70%. Media was changed before transfection. Cell were transfected with the vectors, ΔFGFR1 or L1LE or shL1 or 2605 or 1879 or pLKO.1, along with helper plasmid pCMVΔR8.2 and the

envelope plasmid pMD.G in the proportion of 4:3:1 (20µg:15µg:5µg for cells for a 10cm dish). $CaPO_4$ transfection protocol used was modified from the procedure of Chen and Okayama, 1987 [85]. Plasmids were added to 500µl of $CaCl_2$ (0.25 M), and 500 µl of 2X BBS (pH 7.01) was added drop wise. The precipitate formed after 12 minutes were added to 293T cells. Fresh media was replaced the next day. Cells were allowed to recover for 24-48 hours before collecting media containing the virus . The supernatant was collected and filtered through 0.45 µm filter. The viral supernatant was added to the cell line to be stably transfected. Polybrene was added at a concentration of 10 µg/ml while the
supernatant was added for infection. Cells were incubated overnight and fresh media was added the next day. The cells were selected for puromycin with an initial concentration of 1 µg/ml and finally raising to 10 µg/ml during the subsequent days.

2.5 Western Blots

Cells on culture dishes were rinsed with TBS (Tris-Buffered Saline) and solubilized in RIPA (Radioimmunoprecipitation Assay Buffer) lysis buffer with Complete Mini Protease Inhibitor (Roche # 04 693 159 001) for 2-3 minutes, keeping the plates on ice. The cells were scraped using cell scrapers and lysates were clarified by sonication (vial containing lysate were kept on ice while sonicating).

Protein quantification was performed using the BCA Assay (Thermo Scientific). Equal amounts of 20-30 µg of protein was used to load lanes on the gel. The samples were prepared by adding NuPage 4X LDS sample buffer (Invitrogen) and NuPage 10X reducing agent (Invitrogen) and heated to boiling temperature for 10 minutes. The samples were centrifuged before loading them on NuPage 4-12%

gradient polyacrylamide gels (Invitrogen) along with protein ladders (Magic Mark XP or See Blue Plus 2 prestained standard, Invitrogen). A potential difference of 120 Volts DC was maintained while running the gel. NuPage MOPS running buffer (Invitrogen) was used.

Polyvinylidene fluoride (PVDF) membrane (0.45 µm, Invitrogen) was used for western transfer and was carried out at 4^{O}C at 30 Volts overnight. 5% nonfat dry milk or 3% Bovine Serum Albumin (BSA), dissolved in Tris-Buffered Saline with 0.01% Tween 20 was used as the blocking reagent. The blots were incubated in primary antibody for 1 hour at room temperature and washed three times with TBS/Tween 20 for 15 minutes each. After incubating the membrane in HRP-conjugated secondary antibody for 45-60 minutes, it was washed three times TBS/Tween 20 and incubated with the substrate (Pierce® ECL Western Blotting Substrate # 32106) for 1 minute. The blots were exposed to Blue Basic Autorad Film (ISC Bioexpress, Kensville, UT) in a dark room at various time intervals.

2.6 Collection of L1LE Conditioned medium

U-118/L1LE cells were used to collect L1LE-rich media. 80% confluent plates were washed with PBS three times and then replaced with 8 ml DMEM supplemented with 0.5% FBS. After 24 hours the media was collected and filtered through 0.45µm filters .

2.7 Cell Count

Cell cultures were split the previous day to 10% confluency. 10 random spots were selected and marked using an Object Marker (Nikon TMS inverted phase contrast microscope). Cell cultures were rinsed with PBS three times before the media

was changed to DMEM containing 0.5% FBS. After 6 hours the first cell count was taken. The cell count was again performed 24 hours after the first cell count was taken. The average of the ratio of the number of cells on Day2/Day1 was statistically analyzed and plotted.

2.8 Cell Cycle Analysis

Cells were rinsed with PBS and incubated with 2ml of 0.05% trypsin for 3-5min at 37°C. Cells were transferred to a 15 ml tube and 2ml of Soybean Trysin Inhibitor/DNAse I. The tube was centrifuged at 800 rpm for 3 minutes at room temperature. The pellet was resuspended in 500 µl PBS and 4.5 ml 70% ethanol and stored at -20^{o}C overnight to 2 days. Cells were centrifuged for 5 minutes at 800 rpm and the pellet was resuspended in 5ml PBS. Cells were again centrifuged and the pellet was resuspended in 1 ml DNA staining solution (200µg/ml of DNAse free RNAse A and 20µg/ml Propidium Iodide in PBS). After the cells were incubated for 30 minutes at room temperature in the dark, they were transferred to a FACS tube and analyzed with a Becton Dickinson FACSCalibur Flow Cytometer. The percentage of cells in different cell cycle stages was determined using ModFit *LT* ^{TM} software.

2.9 Time-lapse microscopy for Cell Motility

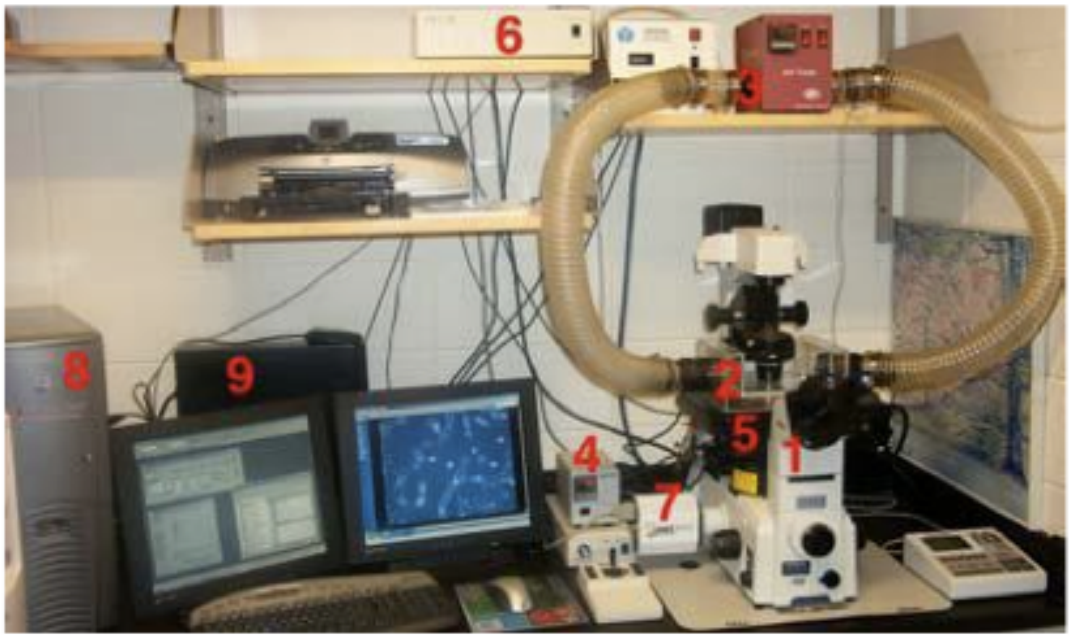

Figure 12 **Components of the custom fully automated time-lapse microscopy system.** 1) Fully automated Nikon TE-2000E with epifluorescence, 2) incubator chamber, 3) WPI temperature controller, 4) Tokai Hit stage insert warmer controller, 5) Prior ProScan II flat-top automated stage, 6) Prior stage controller, 7) Photometrics CoolSNAP ES CCD camera, 8) custom 3GHz computer with 2 gigabytes of RAM, 2 hard drives, dual monitors, and MetaMorph Premier software, 9) uninterruptible power supply capable of running entire system. Out of view is CO2 injection system connected to incubator chamber via tubing (Fotos et al., 2006).

Cell motility analyses of T98G, T98G/shL1, T98G/pLKO.1, T98G/ΔFGFR1, T98G/2605, T98G/shL1/ΔFGFR1, T98G/pLKO.1/2605, U118, U118/L1LE, U118/1879, U118/ΔFGFR1, and U-118/2605 were performed as previously described [86][87]. Confluent cells, grown in 60 mm dishes were "wounded" by introducing scratches using a sterile plastic 1ml pipettor tip. 0.5% serum-containing DMEM media was added after the cells were rinsed three times with HBSS (Hank's balanced salt solution). For inhibitor blocking experiments, the appropriate amount of substance was added to the plates along with the media. After 6 hours, cultures were placed into a custom culture chamber mounted on a ProScan II automated stage (Prior Scientific, Rockland, MA) on a Nikon TE-2000E microscope. Temperature was maintained at 37^{o}C by a combination of a warm air temperature controller (Air Therm, World Precision Instruments, Sarasota, FL) and thermoelectric warming with an optically clear temperature controlled stage insert (Tokai Hit, Shizuoka-ken, Japan). 5% CO_2/95% air was maintained inside the chamber using a gas injection controller (Forma Scientific, Marietta, OH). A CoolSnap ES CCD camera (Photometrics, Tucson, AZ) was used to capture images over the course of the experiment using a Nikon Plan Fluor 10X ELWD objective at areas of interest on each plate for approximately 24h. Phase contrast images were collected at 10 minutes intervals. The system was controlled using MetaMorph Premier Software (Molecular Devices Corporation, Downingtown, PA).

2.10 Analysis of cell motility data

Quantitative analysis of cell motility was performed on acquired sequential phase contrast images using the MetaMorph software "Track Points" feature with nucleoli serving as imaging targets. The resolution of images was converted to 800 X 600 dpi using XnView software. Movies also were made from the stack of images collected every 10 minutes. 25-30 cells per treatment were randomly selected for tracking the position using 'Track Points' tab in MetaMorph software. The paths of different cells were displayed, and the tracking data collected included the velocity, distance and time, which were stored in an excel datasheet for further analysis (e.g. average velocity) [86].

2.11 *In vivo* Chick Embryonic Brain Microinjection

Cells were trypsinized and suspended in cell growth media with 30% Matrigel (Becton Dickinson). The cell density for injection was 2.9 $X10^4$cells/ml. Fertile White Leghorn chicken embryos were obtained from the University of Delaware Department of Animal and Food Sciences. Eggs were incubated in a humidified forced-draft incubator at 37.5°C. On embryonic day 5 (E5), chick embryonic OT (optic tecta, midbrains) were injected with T98G cells. The experimental procedure was detailed previously [88]. Briefly, a small window was cut over the air space at the top end of the eggs and approximately 10 µl of cell suspension (*10^5 cells) was microinjected into the OT using a PV830 pneumatic picopump

(World Precision Instruments; Sara- sota, FL). After injection, sterile ampicillin was added over the embryo, the window in the egg shell was sealed with transparent tape, and the embryo was placed back into the egg incubator until E9.

At E9, the embryos were sacrificed and brains were dissected. E9 chick embryo tecta were fixed in 2% paraformaldehyde in PBS for 2 h, rinsed in PBS and cryoprotected in 30% sucrose overnight. The next day, tecta were embedded in Tissue Freezing Media (cat. # H-TFM; Triangle Biomedical Sciences, Durham, NC) before being sectioned at 10 μm. The cryosections were used for immunostaining for L1. The dissected E9 chick brains also were fixed in 2% paraformaldehyde in PBS overnight and the next day were embedded in 3.5% agar and 8% sucrose in PBS and sectioned at 200 μm using a Vibratome Series 1000 Sectioning System (Ted Pella, Redding, CA) for observation using a Nikon SMZ-1500 zoom stereomicro- scope equipped with epifluorescence attachment and Tucsen color CCD camera (Tucsen Image Technology Inc., Fuzhou, FuJian, China) and for confocal microscopy observation.

2.12 Statistical Methods

Data presented are mean ± SEM of at least three repeats. Student′s t-test was used to analyze difference between two groups. ANOVA was used when more than two groups were involved, and then Student's t-test was further applied to analyze difference between groups. * or #, $P < 0.05$ was considered as significant; **, $P < 0.01$.

Chapter 3

RESULTS

T98G and U118 cells were engineered to create the following cell lines as mentioned in table 2.

Table 2 Stable cell lines created through Lentiviral vector infection

Cell line	Control Cell line
T98G/ΔFGFR1 (FGFR1-)	T98G/2605 (FGFR+)
U118/ΔFGFR1 (FGFR1-)	U118/2605 (FGFR+)
T98G/shL1 (L1-)	T98G/pLKO.1 (L1+)
T98G/ΔFGFR1/shL1 (FGFR1-, L1-)	T98G/2605/pLKO.1 (FGFR+, L1+)
U118/L1LE (L1+)	U118/1879 (L1-)

3.1 Characterization of FGFR1, L1CAMand ADAM10 in glioma tissues

To determine the L1CAM expression level in glioma surgical samples, I used Oncomine (http:// www.oncomine.org) to examine microarray results obtained by Sun et al. [98] on patients with different stages of glioma. As shown in Figure 13, COPA outlier analysis on mRNA levels of 19,574 measured genes from 81

glioblastoma samples and 23 normal brain samples identified FGFR1 among the top 7% genes that are over-expressed, ranking it 3818 at 75th percentile and 2078 at the 95th percentile threshold. The resultant graph clearly shows the increase in the expression level of FGFR1 in all the glioblastoma regardless of the grade compared to the normal brain tissue. With the same dataset, when the gene expression profile for ADAM10 was analyzed based on glioma grade, there was a gradual increase in the expression level of ADAM10 from grade II to the maximum expression at grade IV (Figure 14). With the same dataset, when the expression profile of L1CAM was analyzed, the data showed a decrease in the expression level of L1CAM as the glioma progresses from Grade II to Grade IV (Figure 15).

These analyses suggest that FGFR1 may play a role in glioma progression. The decrease in L1CAM and increase in ADAM10 correlated with the glioma progression could be due to facilitate less adhesion and more cleaving of cell adhesion molecules, which would act as an effective ligand for glioma activity.

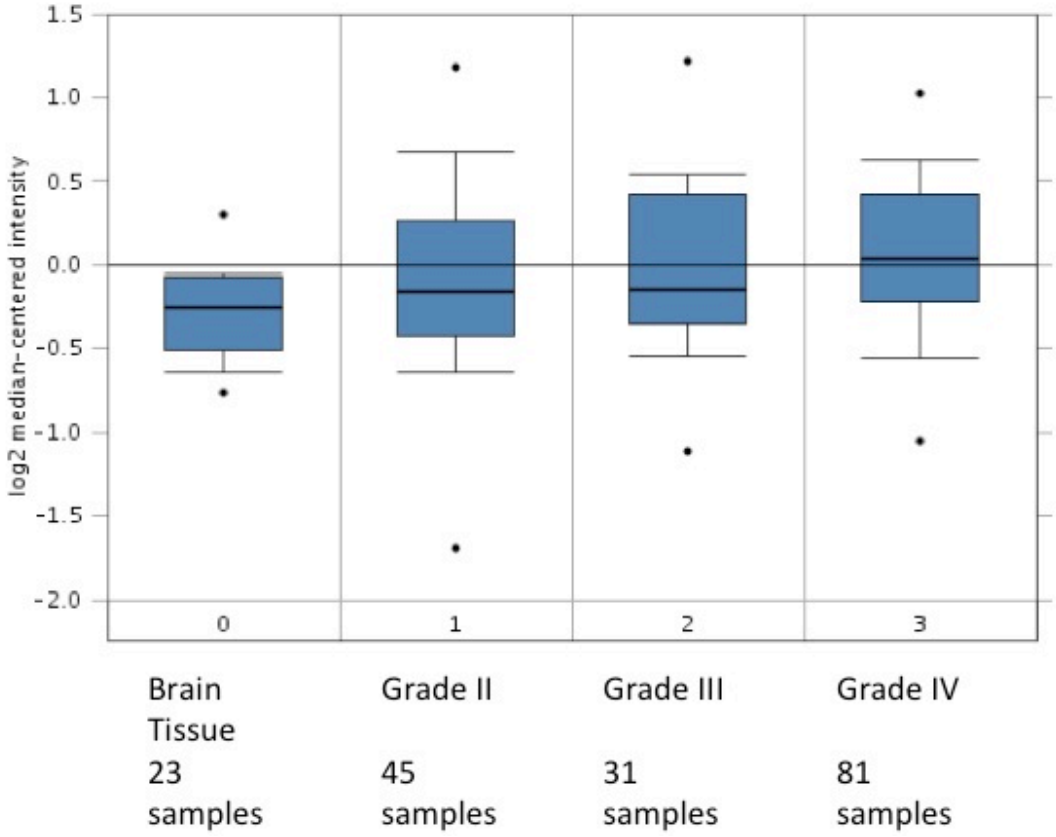

Figure 13 **Characterization of FGFR1 expression in glioma.** ONCOMINE gene microarray database was explored for FGFR1 gene expression in glioma and the results of Sun et al. [98] were displayed by different stages. There was a 1.433-fold increase in the expression level, ranking FGFR1 1295 as top 7% genes over expressed among 19,574 measured genes on mRNA level (http://www.oncomine.org/). Each box represents multiple samples from one class. The stars on the top and the bottom of each bar represents the maximum and minimum value respectively. Each bar displays 90^{th}, 75^{th}, median, 25^{th} and 10^{th} percentile values.

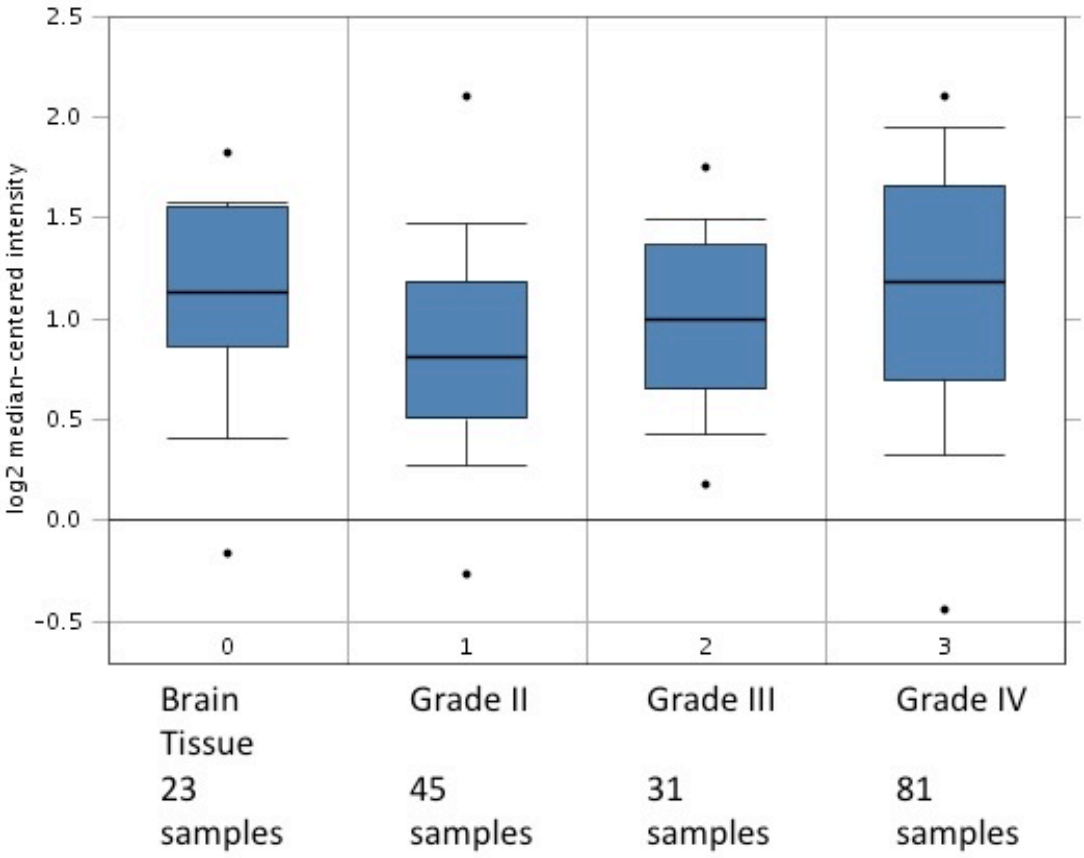

Figure 14 **Characterization of ADAM10 expression in glioma. ONCOMINE gene microarray database was explored for ADAM10 gene expression in glioma and the results of Sun et al. [98] were displayed by different stages. (http://www.oncomine.org/).** Each box represents multiple samples from one class. The stars on the top and the bottom of each bar represents the maximum and minimum value respectively. Each bar displays 90th, 75th, median, 25th and 10th percentile values.

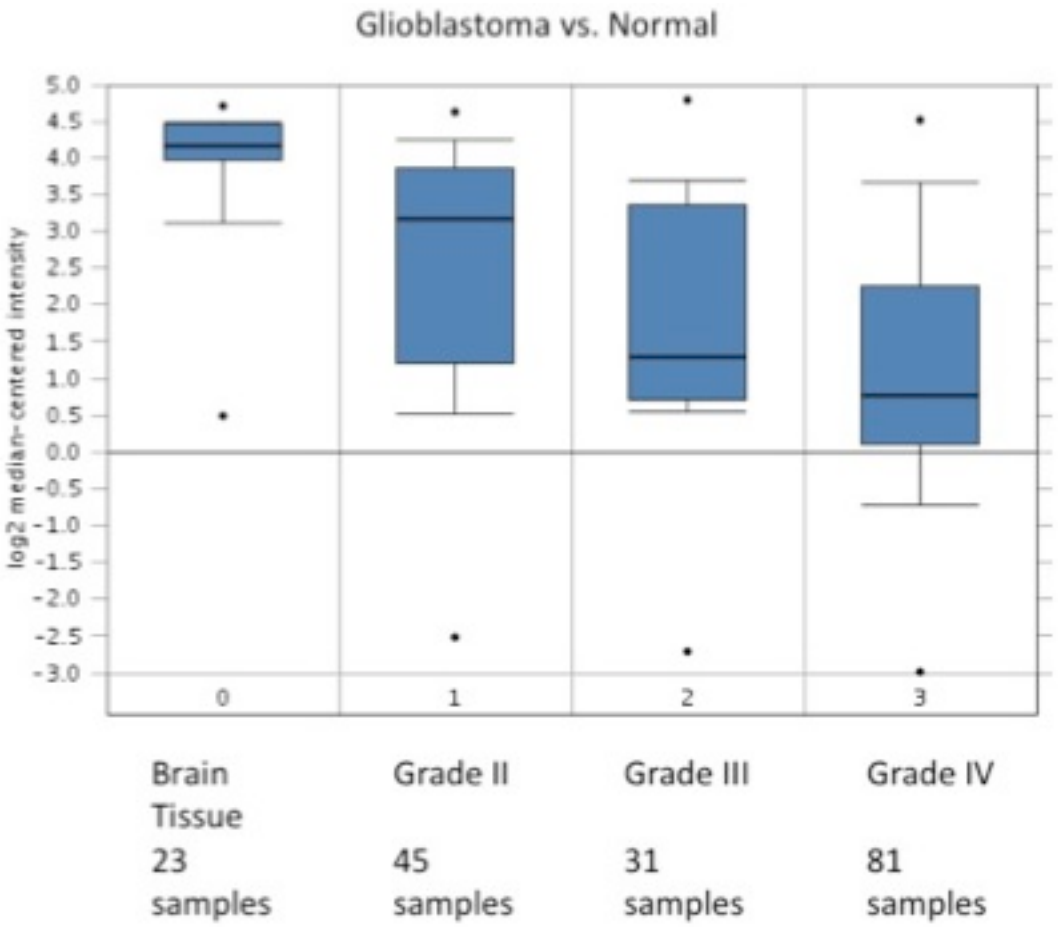

Figure 15 **Characterization of L1CAM expression in glioma. ONCOMINE gene microarray database was explored for L1CAM gene expression in glioma and the results of Sun et al. [98] were displayed by different stages. (http://www.oncomine.org/).** Each box represents multiple samples from one class. The stars on the top and the bottom of each bar represents the maximum and minimum value respectively. Each bar displays 90th, 75th, median, 25th and 10th percentile values.

3.2 Ectopic L1 ectodomain expression results in increased cell migration and invasion

3.2.1 Creation of stable cell lines of U118 expressing L1CAM

Grade III glioma cell line U-118 MG in its native form does not express detectable L1 protein (Yang 2011). Ectopic L1 (L1LE) expressing U-118 (U-118/L1LE) was created by infecting cells with an L1LE sequence incorporated retroviral vector (1879). The control cell lines U-118/1879 were created by infecting U-118 with the empty vector 1879. Western blot performed using UJ127 showed the presence of L1LE expressed by the cells at around 200-220 kDa (Fig 16). β-Actin was used as the internal loading control, which is a housekeeping protein present in presumably equal amount in the entire cells. The antibody for β-Actin produces a band of about 42 kDa.

3.2.2 Super Scratch assay

A *Super Scratch* assay [86] was performed in order to quantify the motility difference between U-118/L1ED and U-118/1879. It was conducted over 24 hours taking images every 10 minutes. 30 cells were tracked using 'Track Points' feature in MetaMorph software. The velocity of each cell was converted to microns/minute. The overall average velocity of each cell was calculated and plotted. There was an approximately 69% increase in motility for U-118 cells expressing L1LE (Fig. 17) The value obtained was statistically compared using students T Test and the P value obtained was less than 0.001, which shows that the data obtained was statistically significant. This shows that cells when they start expressing L1 tend to increase its motility.

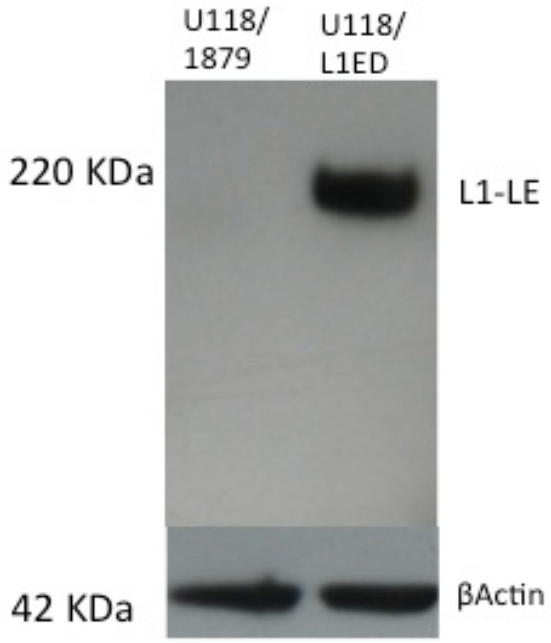

Figure 16 **L1LE expression on U-118 cells infected with L1LE lentiviral vector.** U-118/L1LE and U-118/1879 cell extracts were probed against UJ127 antibody. β actin housekeeping protein was used as a loading control.

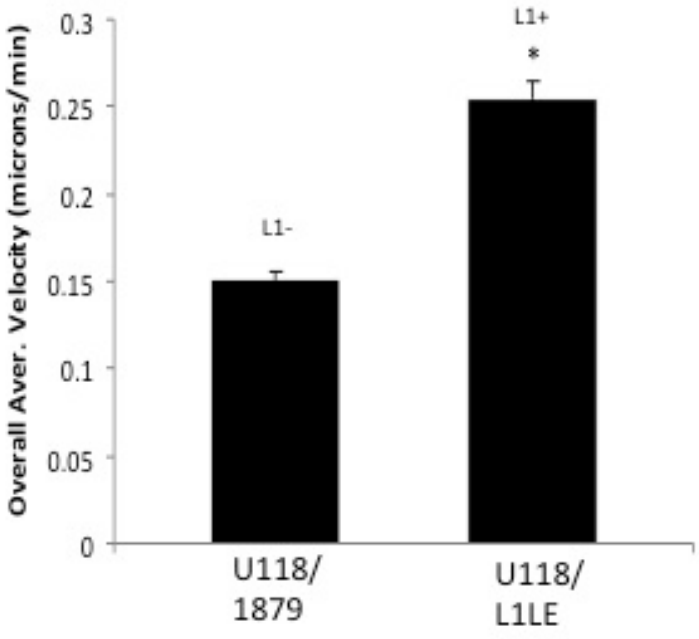

Figure 17 L1LE expression increased U-118 cell motility.
The overall average velocities were calculated using all individual cell velocities collected during the course of the experiment and graphed as single values for the two populations of cells. U18/1879 cell velocity was 0.151 μm/min. and U-118/L1LE cell velocity was 0.255 μm/min. *, $p<<0.001$ in comparison with the average cell velocity of control cell. The results are the mean $\pm$ s.e.m. performed in triplicate.

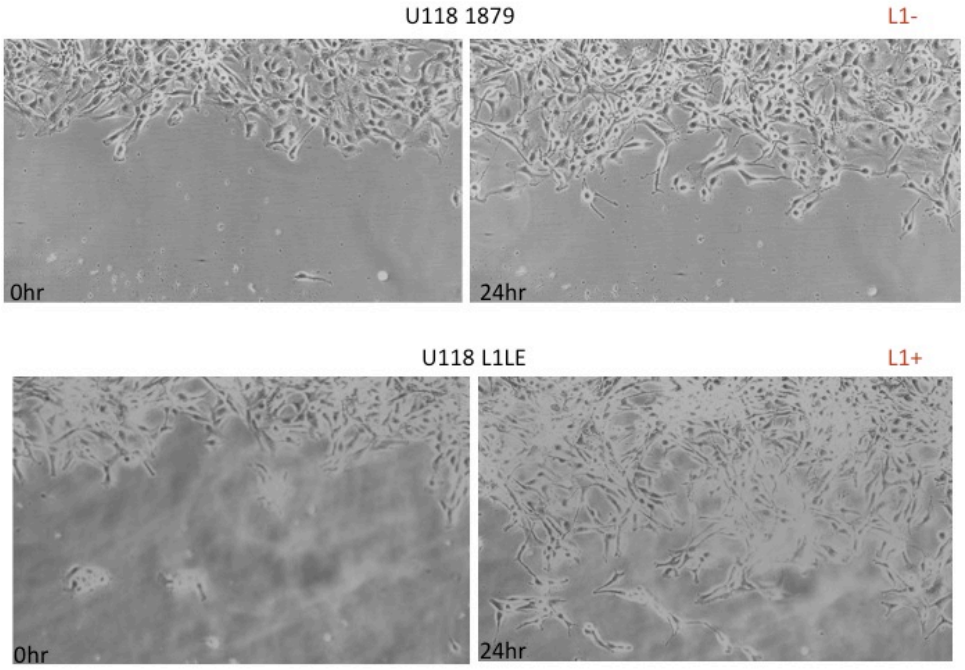

Figure 18 **Cell motility images of U-118/L1LE and U-118/1879.** Scratch was made after media was replaced to 0.5% FBS containing DMEM. Images were captured every 10 minutes over a time interval of 24 hours.

3.3 L1 increases the rate of proliferation of glioma cells

Cell count and cell cycle analyses of propidium iodide stained cells were employed to examine the rate of proliferation of glioma cells. T98G and U-118 ells were manipulated to attenuate and overexpress L1 respectively.

3.3.1 Creation of L1-attenuated T98G glioma cell

T98G/shL1 (L1 short hairpin RNA) cells were created by infecting T98G cells with a lentiviral vector carrying the shRNA for L1. Western blot and immunostaining analyses with anti-L1 antibodies analyzed through FACS confirmed

the inhibition of L1 expression. Control cell line, T98G/pLKO.1, was created by infecting T98G cells with the empty vector pLKO.1. UJ127 antibody staining of western blots showed the absence of the band near 220 kDa corresponding to that of L1CAM compared to the control cell line, T98G/pLKO.1. This shows that shRNA employed to knockdown L1 expression in T98G completely eliminates its expression. β-Actin was used as the loading control. The antibody for β-Actin produces a band of about 42 kDa (Fig. 19).

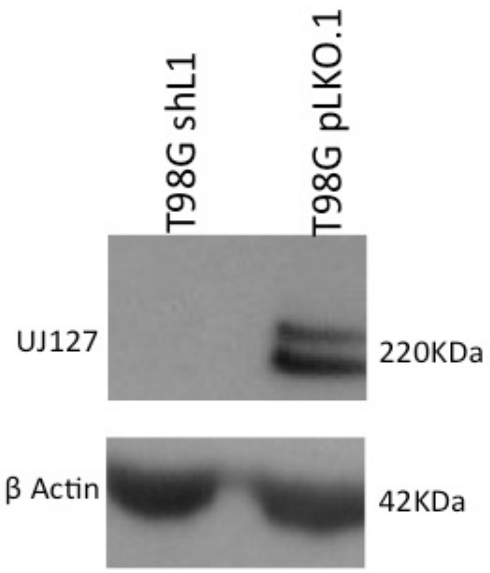

Figure 19 L1 expression on T98G cells infected with L1-targeting shRNA lentiviral vector.
T98G/shL1 and T98G/pLKO.1 cell extracts were probed using UJ127 antibody. β actin is the housekeeping protein used as loading control**.**

3.3.2 Cell count to determine cell proliferation

T98G/pLKO.1 and T98G/shL1 or U-118/L1LE and U-118/1879 cells were used for this analysis. The media was changed to DMEM containing 0.5% FBS and the first cell count was taken after 6 hours. Subsequent cell count was taken after 30 hours. Ratio of cell count on each spot of day 2 by day 1 was determined and the overall average ratio was plotted. T98G/shL1 exhibited a 41% decrease in cell count compared with T98G/pLKO.1 control cells. U-118/L1LE cells showed a 47% increase in cell proliferation rate compared to control cells. The value obtained was statistically compared using students T Test and the P value obtained was less than 0.05, which shows that the data obtained was statistically significant (Fig. 20-21).

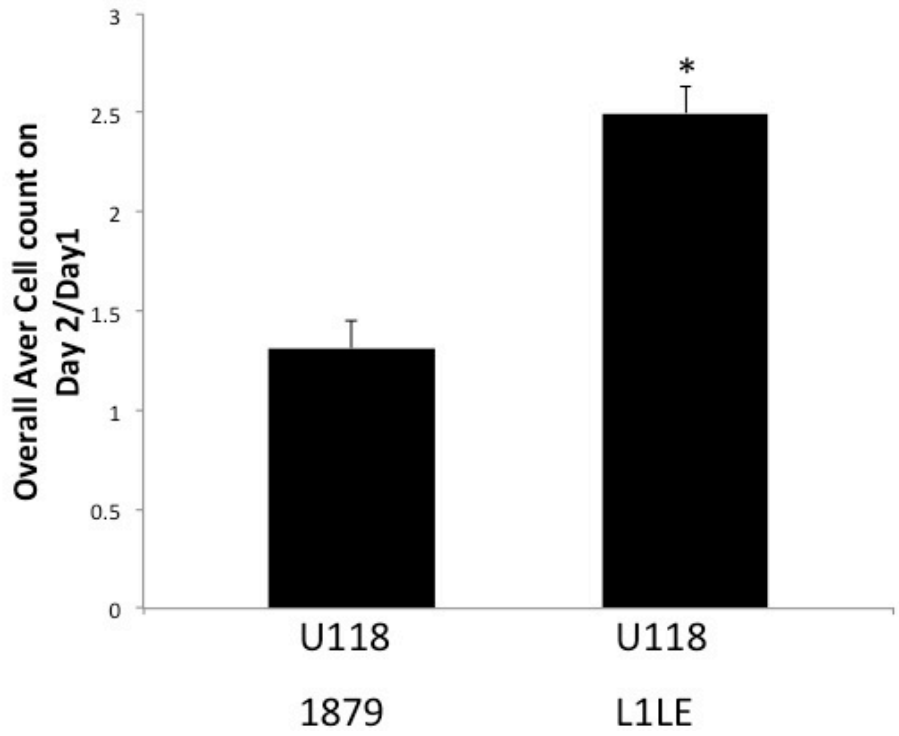

Figure 20 **Overall average cell count on day2/day1 for U-118/1879 cells vs. U-118/L1LE.** Ratio of cell count over ten spots on two consecutive days was determined and plotted. U-118/1879 cell count ratio was 1.311 and U-118/L1LE cell count r. *, $p<<0.001$ in comparison with the average cell count ratio of control cell. The results are the mean $\pm$ s.e.m. performed in triplicate.

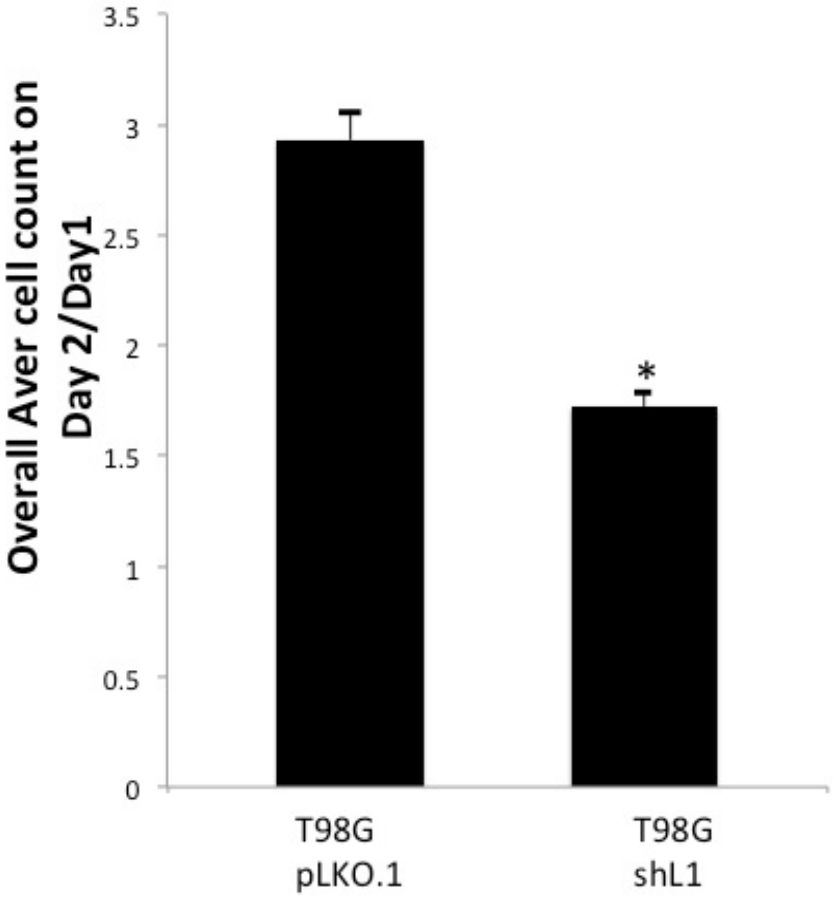

Figure 21 **Overall average cell count on day2/day1 for T98G/pLKO.1 cells vs. T98G/shL1.**
Ratio of cell count over ten spots on two consecutive days was determined and plotted. T98G/shL1 cell count ratio was 2.931 and T98G/pLKO.1 cell count ratio was 1.723. *, $p<0.01$ in comparison with the average cell count ratio of control cell. The results are the mean $\pm$ s.e.m. performed in triplicate.

3.3.3 FACS analysis to determine cell cycle

Cells grown in DMEM containing 0.5% FBS were trypsinised, fixed and stained with propidium iodide**.** Cells were analyzed using FACS (flow cytometry) to determine DNA content. Cell cycle data was then analyzed in ModFit *LT* ™ that differentiates the DNA content graph into the different cell cycle phases. Taking S phase into account for considering the proliferation rate of the cells, T98G/shL1 had only 12.4% s-phase while L1-expressing T98G/pLKO.1 had 23.3% s-phase. U-118 /L1LE had an 27.8% s-phase while U-118/1879, which does not make L1, had only 13.9% s-phase. Each analysis was carried out at least three times. The mean values of the percentage of s-phase between T98G/shL1 and T98G/pLKO.1 or U-118/1879 and U-118/L1LE was then statistically evaluated using Student's T test and the P value was found to be less than 0.05% (Fig. 22) (Fig. 23).

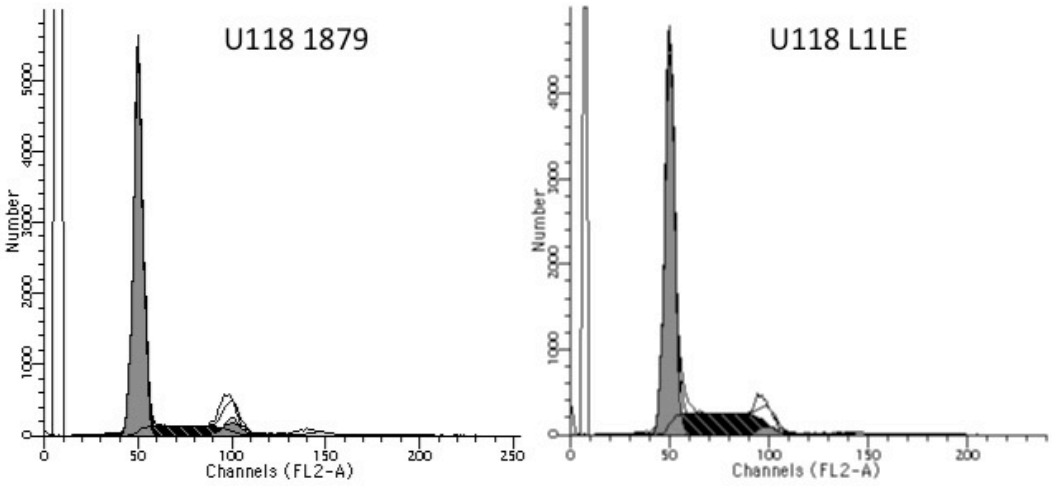

Figure 22 **Cell cycle histogram of U-118/1879 and U-118/L1LE cells**. Cells analyzed by flow cytometry and the percentage of cells in different cell cycle stages was determined using ModFit *LT* ™. Histograms show relative DNA content (x axis) versus cell number (y axis). A) Cell cycle histogram of U-118/1879 cells B) cell cycle histogram of U-118/L1LE cells.

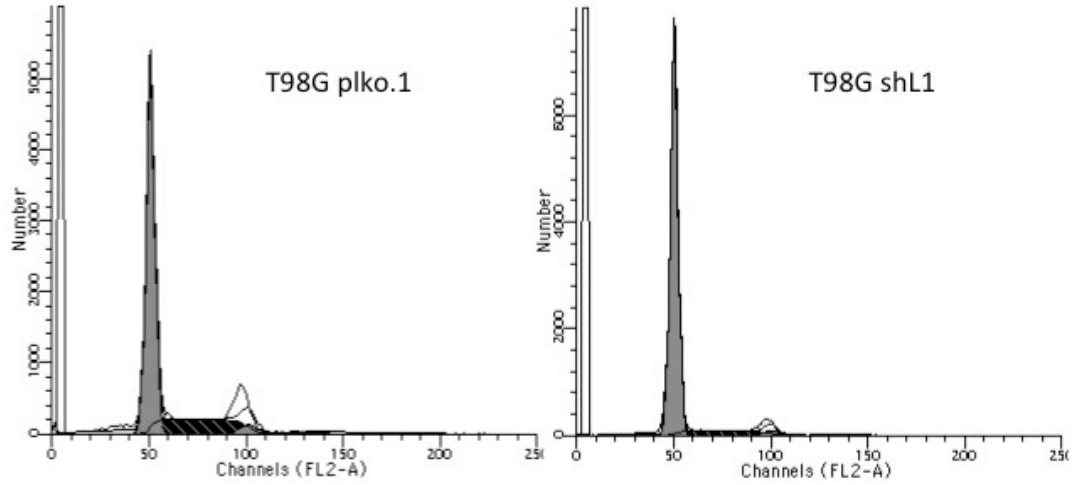

Figure 23 **Cell cycle histogram of T98G/pLKO.1 and T98G/shL1 cells.** Cells analyzed by flow cytometry and the percentage of cells in different cell cycle stages was determined using ModFit *LT*™. Histograms show relative DNA content (x axis) versus cell number (y axis). A) Cell cycle histogram of T98G/pLKO.1 cells with an s-phase of 23.275% B) cell cycle histogram of T98G/shL1 cells with an s-phase of 12.41%**.**

Table 3 **Effect of L1CAM on cell cycle of glioma cells.** Values are determined by taking the average of percentage of cells at different phases of multiple experiments ± s.e.m.

	G0 G1%	S%	G2%
T98G pLKO.1	75.22 ±0.09	23.275 ± 0.125	5.54 ± 1.07
T98G shL1	82.48± 1.764	12.41 ± 0.951	7.88 ± 0.445
U118 1879	80.23±1.568	13.9±0.643	5.87±1.49
U118 L1LE	69.27±1.46	27.795±1.59	2.94±0.13

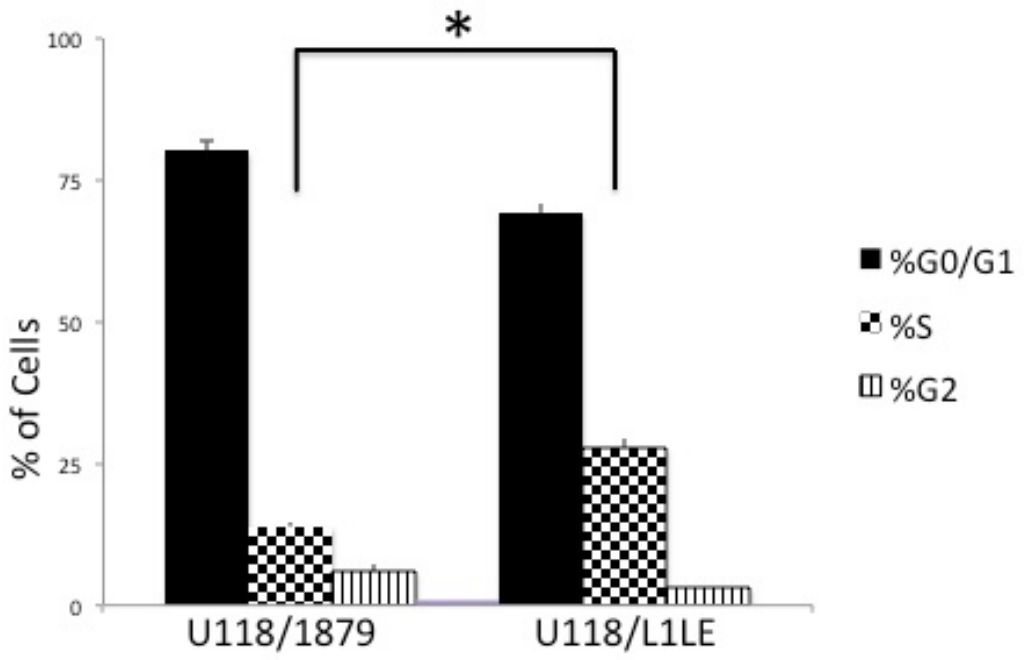

Figure 24 **Quantitative data of cell cycle distribution in U-118/1879 and** U-118/L1LE cells. *, $p < 0.05$ in comparison with s-phase of control**.** The results are the mean $\pm$ s.e.m. performed in triplicate.

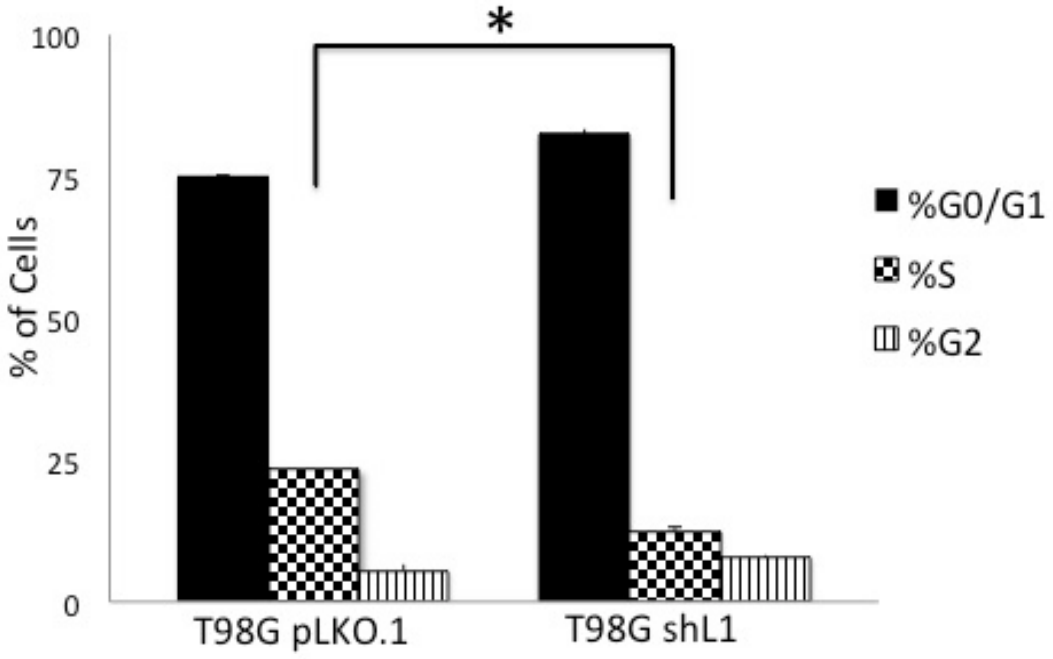

Figure 25 Quantitative data of cell cycle distribution in T98G/pLKO.1 and T98G/shL1 cells. *, $p < 0.05$ in comparison with s-phase of control**.** The results are the mean ± s.e.m. performed in triplicate.

3.4 FGFR1 inhibitor PD173074 affects glioma cell behavior in a dose dependent manner

Since L1 was found to have an effect on glioma cell migration and proliferation (previous 2 results), and L1 has an affinity for FGFR, I used PD173074 to see the contribution of FGFR1 in glioma progression. Migration rate and cell cycle analysis was determined using the SuperScratch Assay and propidium iodide staining respectively on T98G and U-118 cells treated with 50 nM, 100 nM or 1000 nM of PD173074.

3.4.1 Effect of PD173074 on glioma cell migration

PD173074 specifically blocks the phosphorylation of FGFR1 with a half maximal inhibitory concentration (IC50) value of 21.5 nM. T98G and U-118 cells were washed three times with PBS and media was replaced with DMEM containing 0.5% FBS. Plates were then taken for time-lapse analysis for 24 hours, where images were taken every 10 minutes. I used 50 nM, 100 nM and 1000 nM of PD173074 to determine its effect on cell migration at levels specific to FGFR1 and beyond.

T98G cells treated with 50 nM of the inhibitor resulted in an approximately 43% reduction in migration rate compared to DMSO treated control cells. 50 nM and100 nM drug treated cells did not have a significant difference in their rate of migration between each other, while cells treated with 1000 nM had a an approximate 77% reduction in migration rate (Fig. 26).

U-118 cells treated with 50 nM or 100 nM of the inhibitor resulted in only an approximately 25% reduction in migration, while 1000 nM treated cells had 55% reduction in migration rate (Fig. 27). Cells treated with 50 nM did not show a difference in migration rate when compared to cells treated with 100 nM. With the inhibitor treatment at 50 nM or 1000 nM, T98G cells, which make their L1 and FGFR had a higher reduction in migration rate than U-118 cells, which do not express L1 although it make FGFR.

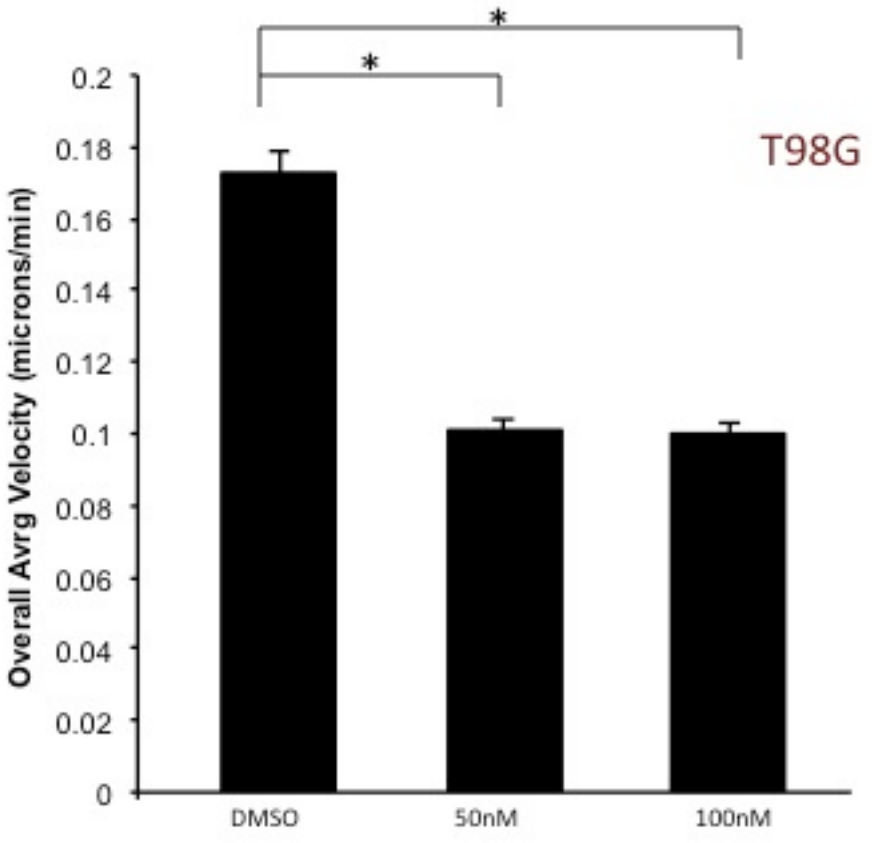

Figure 26 PD173074 decreased T98G cell motility at doses specific for FGFR1 inhibition.

The overall average velocities were calculated using all individual cell velocities collected during the course of the experiment and graphed as single values for the two populations of cells. T98G cells incubated with 50 nM of PD173074 had velocity of 0.172 μm/min, T98G cells incubated with 100 nM of PD173074 had velocity of 0.101 μm/min, T98G control cells had velocity of 0.1 μm/min. *,$p << 0.001$ in comparison with the velocity of control cells. The results are the mean $\pm$ s.e.m. performed in triplicate.

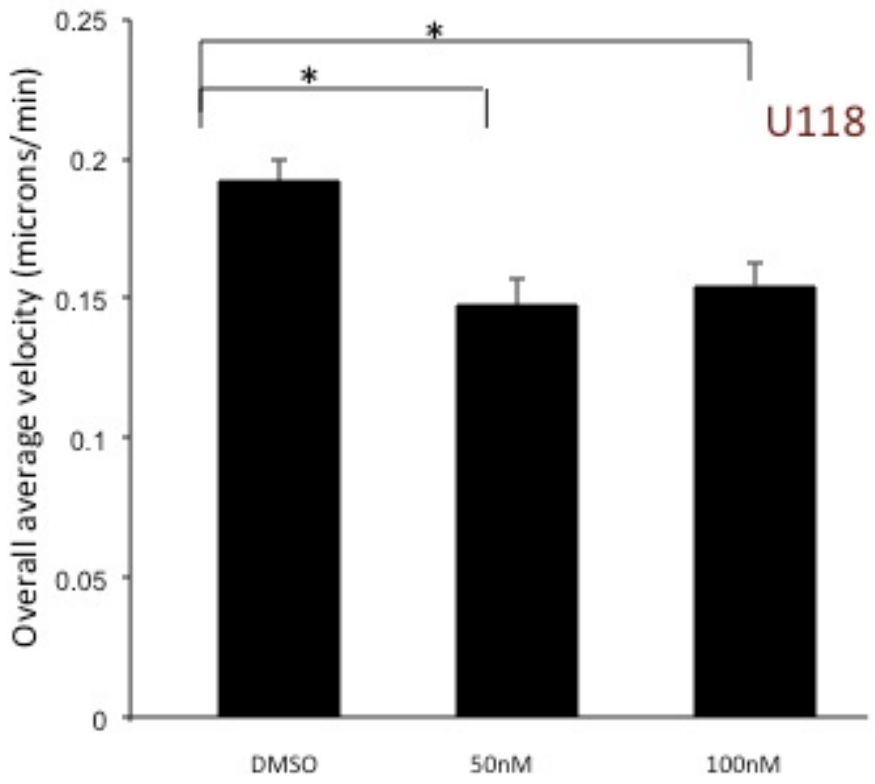

Figure 27 PD173074 decreased U-118 cell motility at doses specific for FGFR1 inhibition.

The overall average velocities were calculated using all individual cell velocities collected during the course of the experiment and graphed as single values. U-118 cells incubated with 50 nM of PD173074 had velocity of 0.147 μm/min, U-118 cells incubated with 100 nM of PD173074 had velocity of 0.155 μm/min, U-118 control cells had velocity of 0.192 μm/min. *,$p<<0.001$ in comparison with the velocity of control cell. The results are the mean $\pm$ s.e.m. performed in triplicate.

3.4.2 Effect of PD173074 on glioma cell cycle

Cells grown in DMEM containing 0.5% FBS was trypsinized, fixed and stained with propidium iodide as described**.** Cells were analyzed using FACS. Cell cycle data was then quantified in ModFit *LT* ™ that differentiates the graph into the different cell cycle phases. Taking s-phase into account for considering the proliferation rate of the cells, T98G cells incubated with 50nM PD173074 had an s-phase fraction of only 23.8 percent while T98G control cells incubated with DMSO had 40.0 percent s-phase. Thus, there was a decrease of approximately 40% in the s-phase fraction in T98G cells incubated with PD173074 at a concentration specific for FGFR1.

U-118 incubated with PD173074 had 17.8 percent s-phase fraction while U-118 control cells incubated with DMSO had 23.1 percent s-phase. This was a decrease of approximately 22% in U-118 cells incubated with PD173074. Each analysis was carried out at least three times. The mean values of the percentage of s-phase between the cells were then statistically evaluated using student T test and the P value was found to be less than 0.05% (Table 3).

Table 4 **Effect of PD173074 on cell cycle fractions of glioma cells.** Values were determined by taking the means of percentages of cells at different phases of multiple experiments ± s.e.m.

	G1%	S%	G2%
T98G/DMSO	51.93±1.06	40.01±0.5	8.07±0.56
T98G/PD173074	65.48±1.93	23.81±0.1	10.72±1.82
U-118/DMSO	73.59±0.14	23.085±1.1	3.31±1.83
U-118/PD173074	77.93±0.68	17.82±1.77	4.26±1.22

3.5 Construction of glioma cell lines expressing truncated FGFR1

To investigate the role of FGFR1 on glioma cells, I made T98G/dnFGFR1 and U-118/dnFGFR1, which are the stable cell lines of T98G and U-118 expressing truncated FGFR (ΔFGFR) respectively. The ΔFGFR sequence was amplified and inserted into the lentiviral vector Lvv.2605. Supernatants containing the ΔFGFR virus were freshly harvested after 293T transfection, and used to infect plain T98G and U-118 cells. Puromycin selection on those infected cells were performed to establish stable cells constitutively expressing ΔFGFR, having a dominant negative effect on the native FGF receptors and therefore shutting down the activation of the receptor. Figure shows the expression of ΔFGFR in T98G/ΔFGFR and U-118/ΔFGFR cell

lines. T98G/2605 and U-118/2605 are the control cells infected with empty vector Lvv.2605. A mouse monoclonal antibody having affinity towards the extracellular domain of FGFR1 was used and the band corresponding to nearly 54 kDa represents the translated form of the truncated FGFR1 sequence. Native form of the FGFR1 was seen on the blot at around 110 kDa (not shown). An antibody against β-actin was used as the loading control. The antibody for β-actin produces a band of about 42 kDa (Fig. 28).

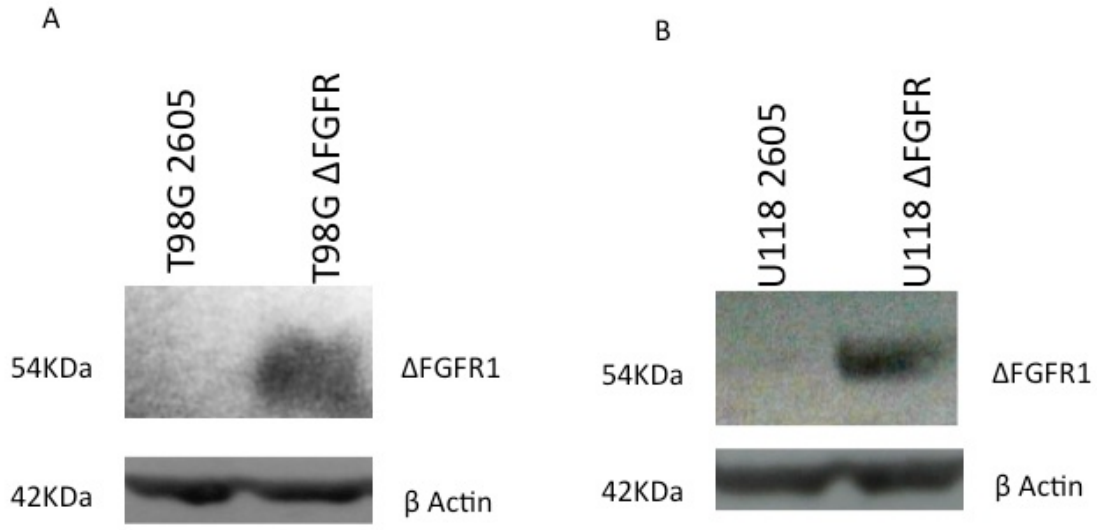

Figure 28 **ΔFGFR1 expression on glioma cells infected with ΔFGFR1 lentiviral vector.** A) T98G/ΔFGFR1 and T98G/2605 cell extracts were probed using an anti-FGFR1 monoclonal antibody. β-actin is the housekeeping protein used as loading control B) U-118/ΔFGFR1 and U-118/2605 cell extracts were probed using the anti-FGFR1 monoclonal antibody. β-actin is the housekeeping protein used as loading control

3.6 Inactivation of FGFR reduces glioma cell proliferation

3.6.1 Cell count to determine the cell proliferation

Glioma cells infected with the different vectors were counted to determine cell proliferation. At least 10 spots were selected and the first cell count was taken after 6 hours. Subsequent cell count was taken after 30 hours. The ratio of cells counted on each spot of day 2 divided by day 1 was determined and the overall average ratio was plotted. T98G/ΔFGFR exhibited an approximate 57% decrease in cell count ratio compared with T98G/2605 control cells. The value obtained was statistically compared using student's T test and the P value obtained was less than 0.05, which shows that the data obtained was statistically significant

U-118/ΔFGFR and U-118/2605 cells also were analyzed similarly. U-118/ΔFGFR showed an approximate 23% decrease in cell proliferation rate (ratio). The value obtained was statistically compared using student's T test and the P value obtained was less than 0.05, which shows that the data obtained was statistically significant. These data show that both T98G and U-118 cells require FGFR signaling for stimulation of proliferation, but that this requirement is greater in T98G cells that express L1CAM (Fig. 29).

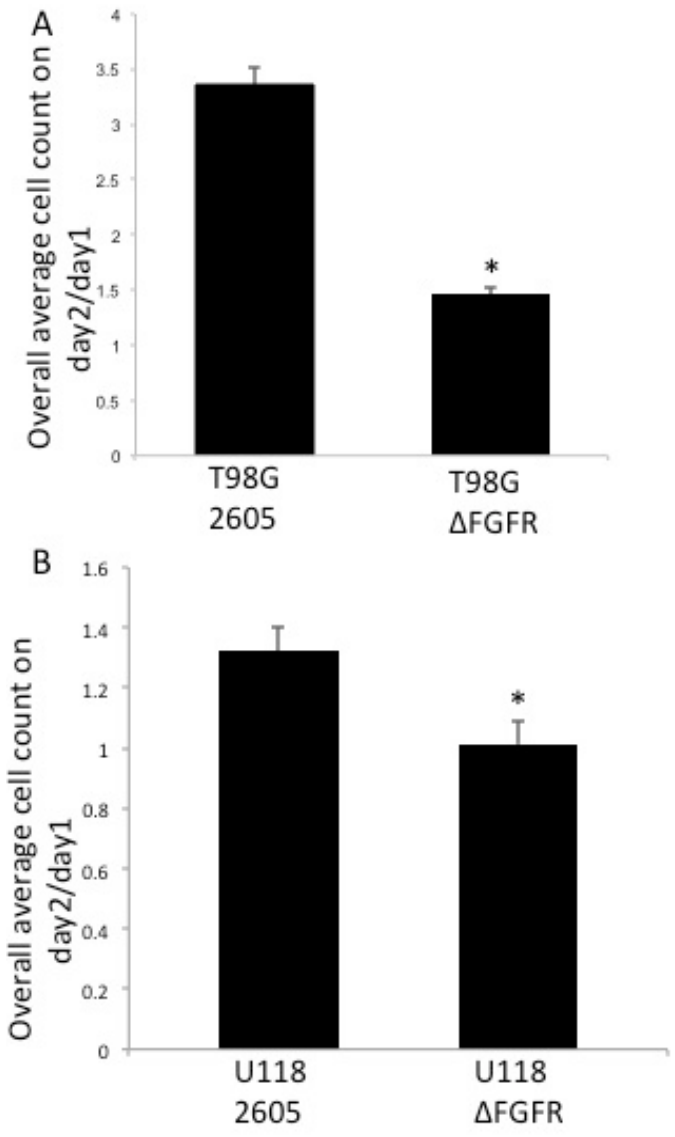

Figure 29 Overall average cell count on day2/day1 for glioma cells lacking FGFR signalling.

Ratio of cell count over ten spots on two consecutive days were determined and plotted. A) T98G/ ΔFGFR1 cell count ratio was 3.2 and T98G/2605 cell count ratio was 1.4. *,$p<<0.001$ in comparison with the cell count ratio of control cell. The results are the mean $\pm$ s.e.m. performed in triplicate.. B) U-118/ΔFGFR1 cell count ratio was 1.0 and U-118/2605 cell count ratio was 1.3. *,$p<0.01$ in comparison with the velocity of control cell. The results are the mean $\pm$ s.e.m. performed in triplicate.

3.6.2 FACS analysis of cell cycle fractions

The second method used to determine potential differences in cell proliferation was a cell cycle analysis of DNA content. Cells were grown in DMEM containing 0.5% FBS, trypsinised, fixed and stained with propidium iodide**.** Cells were analyzed using FACS for DNA content. Cell cycle fractions were then quantified using ModFit *LT* ™ that differentiates the graph into the different cell cycle phases. Taking s-phase into account for considering the proliferation rate of the cells, T98G/ΔFGFR were 12.3 percent while T98G/2605 were 22.7 percent s-phase (Fig. 30).

U-118/ΔFGFR had 18.3 percent s-phase while U-118/2605 had 24.4 percent s-phase. Each analysis was carried out at least three times. The mean values of the percentage of s-phase between T98G/ΔFGFR and T98G/2605 or U-118/ΔFGFR and U-118/2605 was then statistically evaluated using Student's T test and the P value was found to be less than 0.05 (Fig. 31).

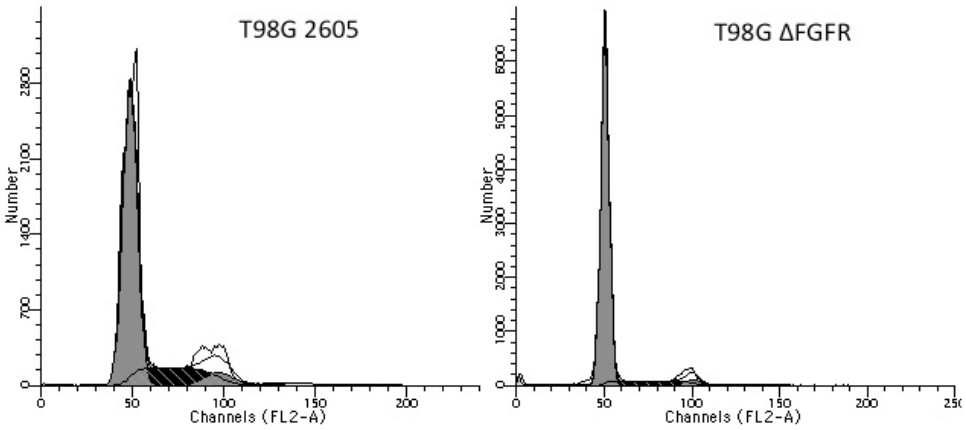

Figure 30 **Cell cycle histogram of T98G/2605 and T98G/ΔFGFR cells.** Cells were analyzed by flow cytometry and the percentage of cells in different cell cycle stages was determined using ModFit *LT*™. Histograms show relative DNA content (x axis) versus cell number (y axis).

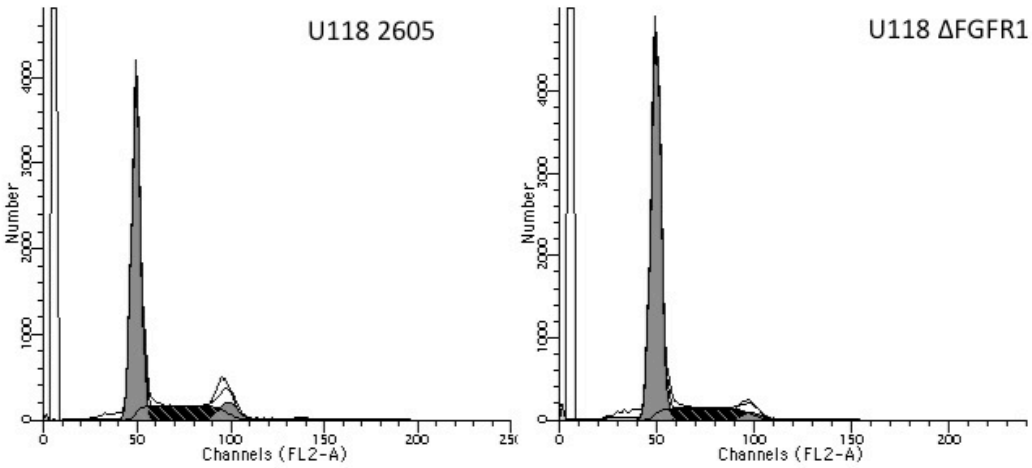

Figure 31 **Cell cycle histogram of U-118/1879 and U-118/ΔFGFR cells.** Cells were analyzed by flow cytometry and the percentage of cells in different cell cycle stages was determined using ModFit *LT*™. Histograms show relative DNA content (x axis) versus cell number (y axis).

Table 5 **Percentage of cells at different cell cycle phases of glioma cells expressing truncated FGFR1 and its control cells.** Values are determined by taking the average of percentage of cells at different phases of multiple experiments ± s.e.m

	G1%	S%	G2%
T98G 2605	73.97±2.08	22.69±0.59	3.34±2.68
T98G ΔFGFR	86.08±1.845	12.33±2.92	1.60±1.075
U118 2605	72.32±2.5	24.44±0.33	3.24±2.54
U118 ΔFGFR	78.61±2.805	18.25±1.44	3.34±0.85

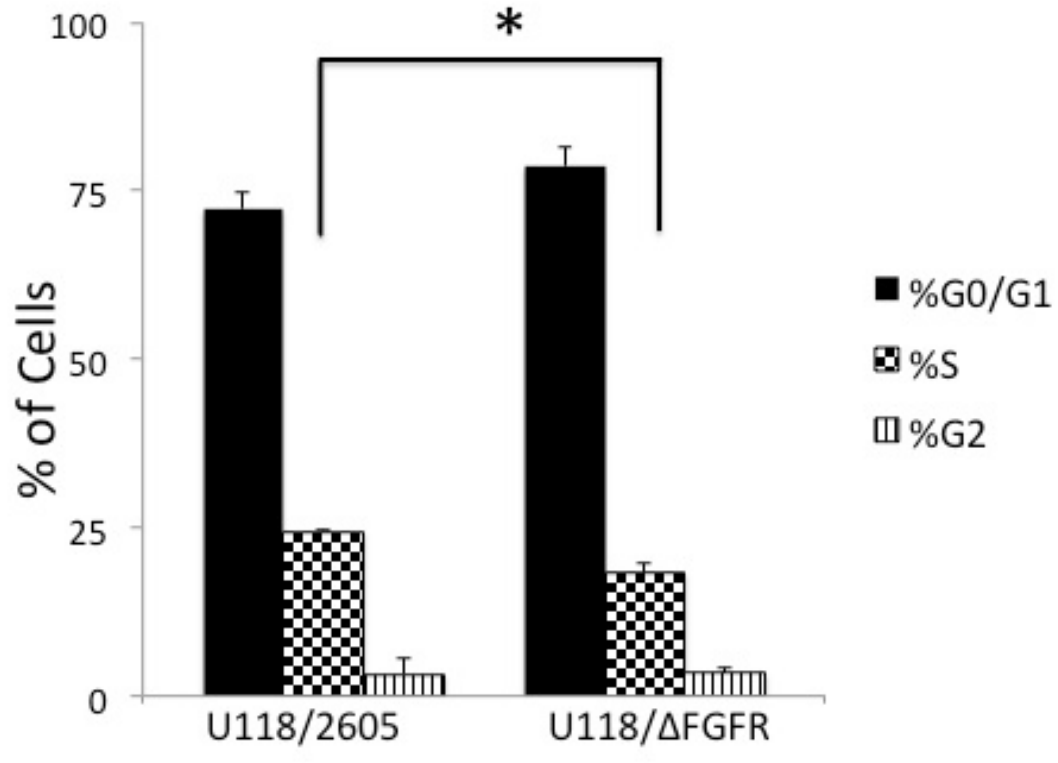

Figure 32 **Quantitative data of cell cycle distribution in U-118/2605 and U-118/ ΔFGFR cells**. *, $p < 0.05$ in comparison with s-phase of control**.** The results are the mean $\pm$ s.e.m. performed in triplicate.

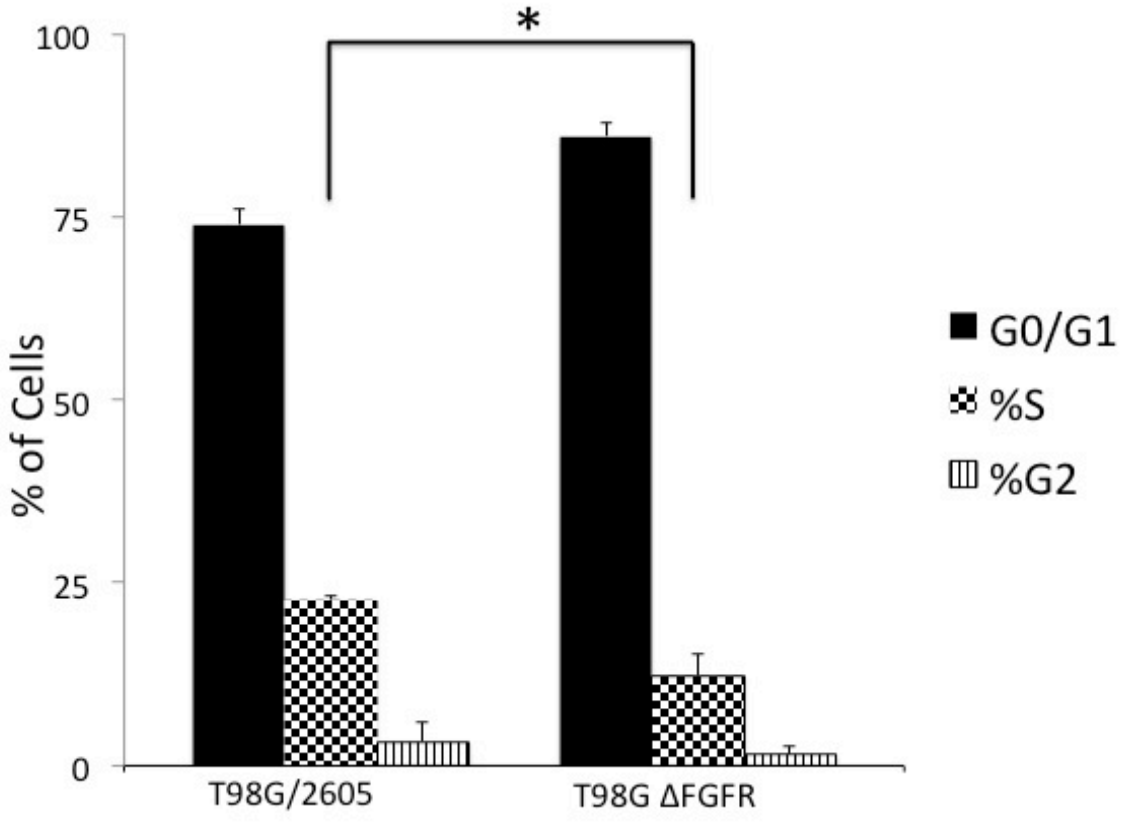

Figure 33 **Quantitative data of cell cycle distribution in T98G/2605 and T98G/ ΔFGFR cells**. *, $p < 0.05$ in comparison with s-phase of control**.** The results are the mean ± s.e.m. performed in triplicate

3.7 Cells expressing truncated FGFR1 exhibit reduced the migration

A *SuperScratch* assay was performed in order to quantify the potential motility difference between T98G/ΔFGFR and T98G/2605. It was conducted over 24 hours taking images every 10 minutes. 30 cells were tracked using 'Track Points' feature in MetaMorph software. The velocity of each cell was converted to microns/minute. The

overall average velocity of each cell type was calculated and plotted. There was an approximate 75% decrease in motility for T98G/ΔFGFR cells compared to T98G/2605 cells. The values obtained were compared using Student's T Test and the P value obtained was less than 0.05, which shows that the difference was statistically significant. The rate of migration of U-118/ΔFGFR and U-118/2605 cells also were compared. There was a decrease of approximately 27% in motility rate between these cell types, and a Student's T Test comparison revealed the P value obtained was less than 0.05, which shows that the differences were significant (Fig. 34).

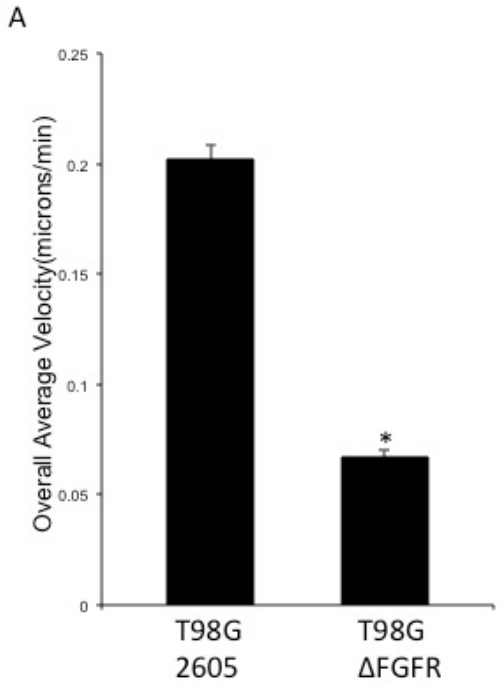

Figure 34 FGFR signaling attenuation decreased T98G cell motility. The overall average velocities were calculated using all individual cell velocities collected during the course of the experiment and graphed as single values for the two populations of cells. T98G/ΔFGFR1 cell velocity was 0.067μm/min and T98G/2605 cell velocity was 0.202 μm/min. *, $p < <0.001$ in comparison with the average velocity of control cell**.** The results are the mean $\pm$ s.e.m. performed in triplicate

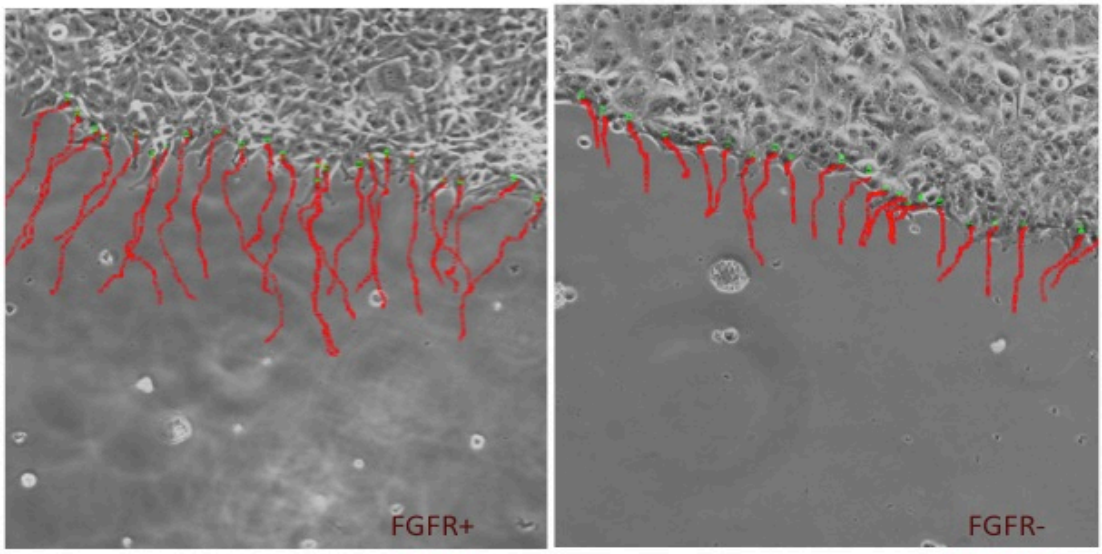

Figure 35 **Cell track images of T98G/2605 and T98G/ΔFGFR1 cell.** Shown is the first image collected during the time-lapse experiment of T98G/2605 and T98G/ΔFGFR1 cells. The red lines are a series of red Xs that denote the position of the cells that were analyzed through each subsequent time-lapse image. Thus, the ends of the red lines in the wound denote the extent of each tracked cell's path at the end of the experiment.

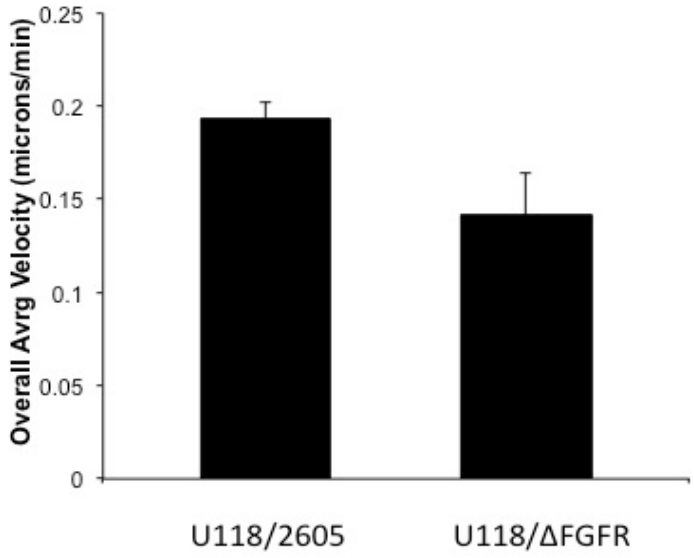

Figure 36 FGFR signaling attenuation decreased U-118 cell motility. The overall average velocities were calculated using all individual cell velocities collected during the course of the experiment and graphed as single values for the two populations of cells. U-118/ΔFGFR1 cell velocity was 0.141μm/min and U-118/2605 cell velocity was 0.193 μm/min. *, $p < <0.05$ in comparison with the average velocity of control cell. The results are the mean ± s.e.m. performed in triplicate.

3.8 L1-FGFR interaction plays a vital role in glioma migration and proliferation

L1 and FGFR have been shown in the previous sections to have significant contribution on glioma cell migration and proliferation. In this section, I have elucidated the effect of L1-FGFR interaction specifically in glioma cell behavior. In order to do that, an FGFR-CHD peptide was used, which presumably binds to L1 and blocks its interaction with FGFRs.

3.8.1 Effect of FGFR CHD peptide on glioma migration

3.8.1.1 Effect of FGFR CHD peptide on T98G cell motility

The rate of migration of T98G cells incubated with FGFR-CHD peptide (peptide A) was compared to T98G cells incubated with scrambled peptide using the *SuperScratch* assay. Cells were washed three times with PBS and media was replaced with DMEM containing 0.5% FBS. Plates were then taken for timelapse analysis for 24 hours, where images were acquired every 10 minutes. After 24 hours the cells were tracked. Analysis showed that T98G cells incubated with the FGFR-CHD peptide had a nearly 50% reduction in migration rate compared to the cells incubated with scrambled peptide (Fig. 37).

3.8.1.2 Effect of FGFR CHD peptide on U118 cell motility

The rate of migration of U-118/L1LE cells incubated with FGFR-CHD peptide (peptide A) was compared with U-118/L1LE cells incubated with scrambled peptide usingthe *SuperScratch* assay. Cells were washed three times with PBS and media was replaced with DMEM containing 0.5% FBS. Plates were then taken for timelapse analysis for 24 hours, where images were acquired every 10 minutes. After 24 hours the cells were tracked. Analysis revealed that U-118 cells incubated with FGFR-CHD peptide had a nearly 24% reduction in migration rate compared to the cells incubated with the scrambled peptide.

U-118/1879 cells also were incubated with peptide A or the scrambled peptide and the rate of migration was not affected. (Fig. 38)

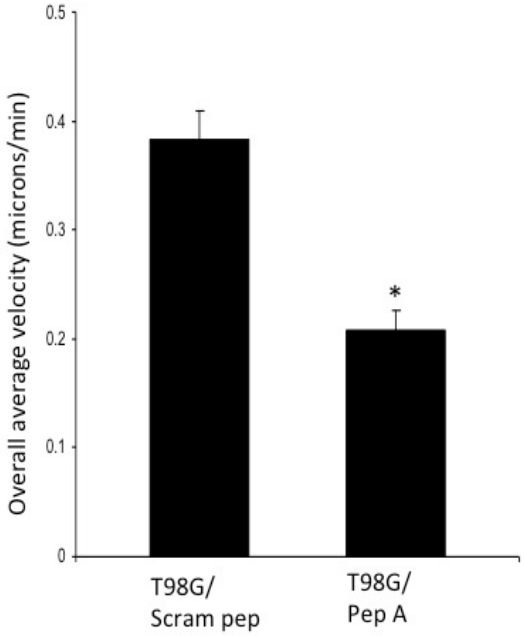

Figure 37 **FGFR-CHD peptide decreased T98G cell migration rate.** The overall average velocities were calculated using all individual cell velocities collected during the course of the experiment and graphed as single values for the two populations of cells. T98G cell incubated with scrambled peptide had an average cell velocity of 0.383 μm/min and T98G cells incubated with FGFR-CHD peptide had an average cell velocity of 0.209 μm/min. *, $p < <0.001$ in comparison with the average velocity of control cell**.** The results are the mean $\pm$ s.e.m. performed in triplicate. Scram pep and Pep A refers to scrambled peptide and FGFR-CHD peptide respectively.

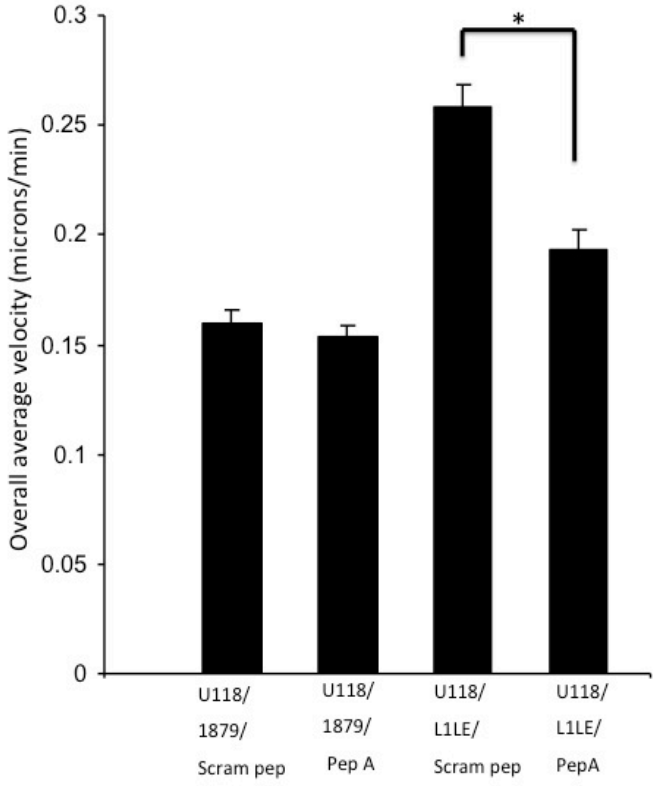

Figure 38 **FGFR-CHD peptide decreases U-118/L1LE cell migration rate.** The overall average velocities were calculated using all individual cell velocities collected during the course of the experiment and graphed as single values for the two populations of cells. U-118/1879 incubated with scrambled peptide or FGFR-CHD peptide did not have a significant difference in their rate of migration. U-118/L1LE cells incubated with scrambled peptide had an average cell velocity of 0.258 μm/min and U-118 cells incubated with FGFR-CHD peptide had an average cell velocity of 0.193 μm/min. *, $p < <0.001$ in comparison with the average velocity of control cell**.** The results are the mean $\pm$ s.e.m. performed in triplicate. Scram pep and Pep A refers to scrambled peptide and FGFR-CHD peptide respectively.

3.8.2 Effect of FGFR CHD peptide on glioma cell cycle

Cells grown in DMEM containing 0.5% FBS was trypsinized, fixed and stained with propidium iodide as described**.** Cells were analyzed using FACS. Cell cycle data was then quantified in ModFit *LT* ™ that differentiates the graph into the different cell cycle phases. This experiment was carried out in two different conditions: 1) confluent cells incubated with the peptide 2) non confluent cells incubated with the peptide. Surprisingly, when the T98G and U-118/L1LE cells were incubated with the peptide when they were not in confluent stage, there was no difference in the S phase between cells incubated with the FGFR-CHD peptide and scrambled peptide for both T98G and U-118/L1LE cells (data not shown). This experiment was repeated three times and was consistent.

Confluent U-118/L1E and U-118/1879 cells were incubated with peptide A or scrambled peptide and the cell cycle data was analyzed. U-118/1879 had 14.9% s-phase, U-118/1879 incubated with scrambled peptide had 13.3%, and U-118/1879 incubated with peptide A had 13.5% s-phase. Thus, there seems to be no difference in the s-phase among these cells when they do not express L1 and, hence, the peptide has no blocking effect. However, U-118/L1LE had an s-phase of 29.4%, U-118/l1LE incubated with the scrambled peptide had 26.2% s-phase, and U-118/L1LE cells incubated with peptide A had a reduced s-phase of 14.9%. This reduced value is close to the s-phase of U-118 cells that do not express L1 (Fig. 39) (Table 5). Since T98G cells attains G_0 phase when they become confluent [115], the effect of peptide on confluent T98G cells cannot be determined.

Table 6 **Percentage of cells at different cell cycle phases of U-118/L1LE and U-118/1879 cells incubated with peptide.**

	G0/G1%	S%	G2%
U-118/1879	79.76	14.94	5.30
U-118 1879 (Scrambled pep)	82.65	13.25	4.10
U-118 1879 (Peptide A)	78.29	13.51	8.20
U-118/L1E	67.81	29.38	2.81
U-118 L1LE (Scrambled Pep))	70.72	26.21	3.07
U-118 L1LE (Peptide A)	80.92	14.93	4.24

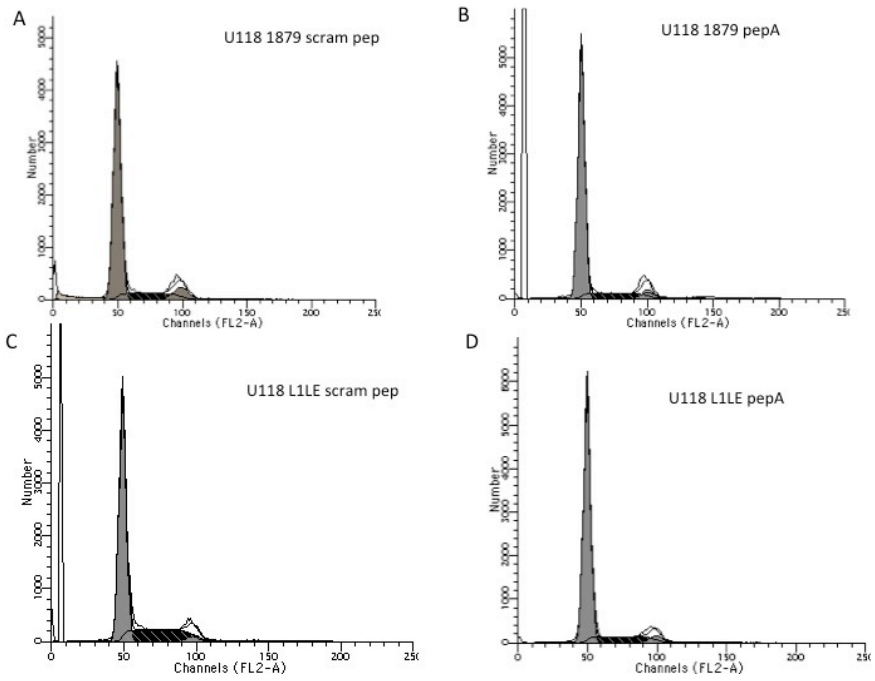

Figure 39 **Cell cycle histogram of U-118/1879 and U-118/L1LE cells incubated with scrambled peptide and FGFR-CHD peptide.** Cells wereanalyzed by flow cytometry and the percentage of cells in different cell cycle stages was determined using ModFit *LT* ™. Histograms show relative DNA content (x axis) versus cell number (y axis).

3.9 Disruption of both L1 and FGFR activity has a drastic reduction in glioma cell migration

The rate of migration of T98G/shL1/ΔFGFR cells were compared with that of T98G/pLKO.1/2605 cells using the *SuperScratch* assay. Cells were washed three times with PBS and media was replaced with DMEM containing 0.5% FBS. Plates were then taken for timelapse analysis for 24 hours, and images were taken at a time interval of 10 minutes. After 24 hours the cells were tracked. It was observed that T98G/shL1/ΔFGFR had nearly 95% reduction in migration rate compared to that of its control cell line that expresses both L1 and FGFR. Thus, when both the L1 and FGFR signaling systems are attenuated, these glioma cells were virtually stopped in their tracks (Fig. 40).

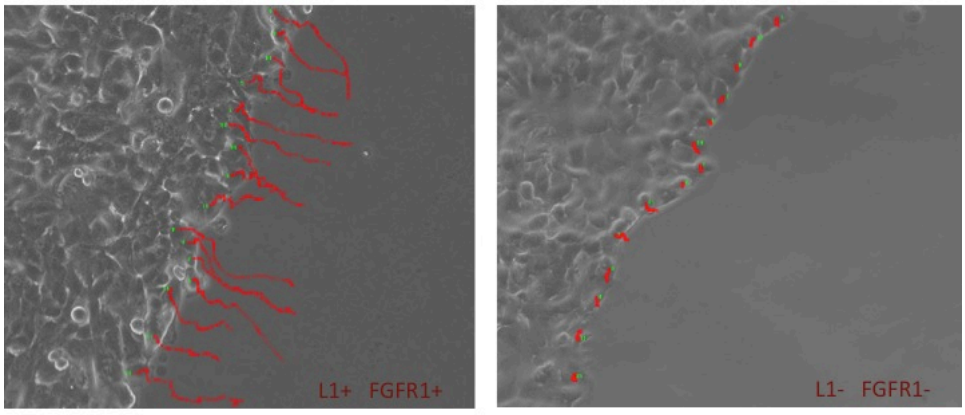

Figure 40 **Cell track images of T98G/pLKO.1/2605 and T98G/shL1/ΔFGFR1 cells.** Shown are the first images collected during the time-lapse experiment of T98G/pLKO.1/2605 and T98G/shL1/ΔFGFR1 cells. The red lines are a series of red "Xs" that denote the position of the cells that were analyzed through each subsequent time-lapse image. Thus, the ends of the red lines in the wound denote the extent of each tracked cell's path at the end of the experiment.

CHAPTER 4

DISCUSSION

Interactions between L1CAM and FGFRs and its implications in neurite outgrowth led me to investigate the effect of this interaction in glioma progression. L1 plays a crucial role during central and peripheral nervous system development, facilitating neuronal migration, neuronal survival, as well as axon outgrowth, guidance, fasciculation, and regeneration. But it also has been studied to be correlated with different kinds of cancers such as, breast, melanoma, lung, colon and ovarian cancer. The aggressiveness of the cancer and bad prognosis is correlated with the expression of L1CAM in several cancers. Overexpression of growth factors or its receptors have been implicated with the dawn of a variety of human cancers. Even though FGFR has been observed to affect tumor size in glioma [64][65][66], the role of FGFR in glioma cell migration and the mechanism underling the activation of the receptor has not been shown until now. The effects shown here of L1-FGFR interaction in playing a crucial role in glioma migration shows that multiple ligands can cause receptor activation, even though FGF has been proposed as the crucial factor for its activation [63][64].

4.1 L1CAM plays a crucial role in glioma proliferation and migration

L1CAM is correlated with the aggressiveness of different types of cancer. Previous studies in our lab has shown the proteolysis of L1CAM and its subsequent release. The reason for increased expression of L1CAM can be explained by

considering the characteristics of L1CAM, for what makes the molecule unique from the rest of its family. Cells make strong contact with the environment through heterophilic binding with other cell adhesion molecules such as cadherins, which is a Ca^{2+} dependent binding molecule. While L1CAM do not require helper ions for interaction, and they contribute more towards the mobility of cells in the niche rather than sticking tendency [90]. This process could be supplementing the glioma cells in processing its immortal nature, thus taking that into consideration, Our lab [118] has shown that L1CAM attenuation leads to approximately 60% reduction in migration rate of T98G cells, which probably is due to decreased focal complex turnover [60]. Also, the invasion study carried out in the chick brain showed that T98G cells with attenuated L1CAM were completely retarded from migrating into the brain paranchyma. Also I have shown that making a glioma cell line ectopically express L1CAM made them highly motile *in vitro.* There was a 69% increase in migration rate of U-118/L1LE compared to that of U-118/1879. I also examined if L1CAM had any effect on glioma cell proliferation. Studies performed by Bao *et.al* [5] suggested an effect of L1CAM on glioma stem cell proliferation. They have shown that glioma stem cells whose L1 expression is knocked down using short hairpin RNA had a reduced tumor size *invivo*. They did not, however, characterize its role in proliferation rate and cell cycle regulation.

I used two different misexpression strategies in order to determine the effect of L1CAM on cell proliferation: 1) by shutting down L1 expression, through shRNA interference, from a cell line which makes L1CAM in full-length form and proteolyzes it to release a long ectodomain (T98G) and 2) by making a cell line express L1CAM ectodomain which does not express it (U-118). As expected, both cell

lines expressing L1CAM exhibited higher rates of proliferation compared to the cell lines that did not express L1CAM, as determined by cell counts. T98G/shL1 exhibited a 41% decrease in rate of proliferation compared to T98G/pLKO.1. U-118/L1LE exhibited a 47% increase in the rate of proliferation compared to U-118/1879. In order to avoid the contribution of molecules from the serum supplement to mask or interfere with effects of L1 on proliferation, the cells were grown in 0.5% serum-containing media while the rate was determined.

Cell cycle data obtained though FACS analysis of propidium iodide stained cells also correlates with the data obtained through cell counts. The percentage s-phase of T98G/shL1 was drastically reduced to approximately 12% compared to that of T98G/pLKO.1 that had approximately 23% s-phase. U-118 cells also displayed the same effect where, U-118/L1LE had approximately 27% s-phase while U-118/1879 had only 13% s-phase. Measurement of s-phase by this method allowed me to accurately predict the percentage of cells undergoing active division under different conditions of L1 expression. However, since L1 signaling could occur through integrins [24] as well as L1 interaction with FGFRs [46], the net effect observed could be the because of interactions with both receptors.

The soluble L1 released after proteolysis from glioma cell surfaces (e.g. T98G) can bind with the similar fashion as cell-surface L1 with integrins such as αvβ3, αvβ5, [54][24] through its RGD motif on the sixth Ig domain. L1 on the cell surface, in its homo – or multi—dimer form recruits integrins to form focal complexes. Even after cleavage this interaction is unaffected. This interaction could occur either in an autocrine or paracrine manner. This leads to the transmission of signaling molecules such as FAK and Src, which further leads to the recruitment of cytoskeleton proteins such as

Ras1 and cdc42 GTPases [91] and regulating actin assembly and cell elongation. My work would further open a new signaling pathway involved in cancer progression, namely one which is transmitted through the FGFR.

4.2 L1 plays a crucial role in FGFR activation in Glioma cells.

FGFRs have been associated with various cancer progression. I have analyzed datasets of clinical samples and found that FGFR1 expression levels were elevated in glioma tumors compared to the normal brain tissue samples [figure]. FGFR1 is in the top 7% of genes that are overexpressed in glioblastoma out of 19,574 genes analyzed. When the expression levels were compared among different grades of glioma, there was not a significant difference between them. When the expression level of FGFR2, the FGFR expressed by normal glia, was analyzed in the clinical sample datasets, glioblastoma (Grade IV) exhibited an under-expression in its level compared to the normal brain tissue (data not shown). This data correlates with previous findings that showed there is expression of FGFR1 in glioma tissues while FGFR2 was absent [63][99]. FGFR1 inactivation has been implicated with a reduction in tumor size [64][65]. There has been no evidence indicating a role of FGFRs in glioma migration. Two approaches have been used to study the effect of FGFR in glioma progression. The dominant-negative strategy has been used for decades to impede the activation of receptors. PD173074, FGFR1 inhibitor drug has also been used to block the receptor activity.

Datasets analyzed from clinical samples shows that there is a gradual increase in the expression profile for ADAM10 protease, which cleaves L1, from grade II to Grade IV of glioma cells. But the expression profile for L1CAM on different grade showed a decrease in the expression profile of L1CAM as glioma progresses.. Since glial cells endogenously do not express L1CAM, the presence of L1CAM on glioblastoma tissues is abnormal. Increased expression of the L1CAM cell adhesion molecule would normally result in the tumor cells tending to adhere with each other and with their environment. But as glioma progresses the decrease in l1CAM expression could be due to facilitate glioma cells to less actively stick with the cells and o increase their tendency to migrate. However, since the glioma cells overexpress the protease ADAM 10, this cleaves the surface L1CAM and stimulates motility and proliferation, partially through FGFRs.

I created a lentiviral vector that carries a sequence for the truncated form of chicken FGFR1 (cek1). Human and chicken FGFR1 amino acid sequences were aligned and the results showed more than 96% identity. Therefore, truncated chicken FGFR1 can be used efficiently to knock down the receptor in human cell lines. The dominant-negative strategy is highly effective in averting the intercellular signaling through the receptor since the activation of the receptor is through cross phosphorylation of ligand bound receptors. Also, if the receptor can under go hetero-dimerization, it can efficiently stop the activity of other isoforms as well. It has been shown that a 10-80 fold increase in the expression of truncated form of FGF1 can interfere with other isoforms of FGFR, which includes FGFR2, FGFR3, and thereby inhibiting the signaling through the entire FGF receptor family [53][55]. Figure 27 shows the expression of the truncated form of the protein.

It has been previously shown that FGF regulates glioma cell proliferation [54]. Cell proliferation data shows that T98G cells expressing truncated FGFR1 had a 57% reduced cell count compared to T98G cells having functional FGFRs. This data is consistent with the cell cycle analysis that showed the s-phase of T98G/ΔFGFR was only 12.33% while T98G/2605 had a higher percentage of 22.69%. This is a clear indication that much of the signaling necessary in T98G cells for cell division is occurring through FGF receptors. But the outcome for U-118 cells were slightly different. The cell count for U-118/ΔFGFR had only a reduction of 23% compared to U-118/2605 cells and this data was supported by the cell cycle data, which showed that the s-phase was reduced from 24.44% to 18.25%. This shows that control of cell proliferation of U-118 cells is less dependent on FGFR signaling compared to that of T98G cells. It may be that more signaling for cell proliferation occurs through integrin receptors.

Glioma cells incubated with PD173074 at a concentration specific to inhibit FGFR1 also had decreased glioma cell proliferation. T98G cells had a decrease of 41%, whereas U-118 had only a decrease of 23% in cell proliferation rate [Table 4]. Since the decrease in proliferation using PD173074 and dominant negative approach were similar, FGFR1 could be the vital molecule in regulating glioma cell proliferation among the four family member receptors. Glioma cells expressing ΔFGFR when xenografted in immunodeficient mice exhibited a decrease in tumor size [64].

Glioma cells expressing truncated FGFR1 displayed a drastic decrease in migration rate. T98G/ΔFGFR had a decrease of 65% compared to T98G/2605, while U-118/ΔFGFR had a decrease of 27% compared to U-118/2605 cells. This data was

consistent when migration was determined for glioma cells incubated with PD173074. Since there was not a complete termination of migration and proliferation there has to be some other major signalling even taking place through the glioma cells, which is likely to be integrins.

FGF has been studied to have a growth promoting effect on glioma cells in a dose dependent manner and further studies implicated that the signaling occurs through the MAP kinase pathway rather than PI3kinase/AKT. This is also correlated with decreased expression of G1-S transition regulating protein such as cyclin D1, cyclin D2 and CDK4. SiRNA against FGFR1 has also been implicated to have a reduction in glioma cell proliferation [63]. Inhibiting the FGF pathway reduced GBM cell growth [101][102]. PD173074 decreased c-MYC levels especially after 72 hours of incubation. Role of c-MYC to induce glioma growth was demonstrated in transgenic mice [104[105]. PD173074 is also found to inhibit breast cancer cell growth [106].

The previous data shows the effect of L1 on GBM cell proliferation. U-118 did not display the as large of a reduction in cell proliferation compared to T98G cells. L1-attenuated T98G cells (T98G/ΔFGFR1) displayed a decrease in cell proliferation rate and migration. What could be the contribution of L1 in FGFR activation? The solution can be found by determining the rate of migration and proliferation through interfering with L1-FGFR interaction specifically. In order to block the L1-FGFR interaction specifically, I used a peptide derived from the CAM Homology Domain (CHD) of FGFR1. FGFR-CHD peptide has been used previously to determine the effect of CAMs signaling via FGF receptors in neurite outgrowth of cerebellar neurons [47]. By using the peptide they found that there was more than 90%

decrease in neurite outgrowth. When I used the peptide derived from CHD specific to L1CAM interaction with FGFR, there was a significant effect on glioma cell migration but not on proliferation. T98G cells, when incubated with the peptide, had a decrease of approximately 48% in migration rate compared to the rate of migration of T98G cells incubated with scrambled peptide. U-118 cells did not show any effect on its migratory effect when incubated with the peptide. The reason is obviously due to U-118's lack of endogenous L1CAM expression, due to which there is no blocking effect of the peptide. But when the peptide was used against U-118/L1LE cells, there was a reduction of 20% in migratory rate compared to U-118/L1LE cells incubated with scrambled peptide. This data clearly show that the disruption of L1-FGFR interaction had a negative impact on glioma cell migration when the cells express L1. In other words, L1-FGFR interaction contributes towards glioma cell motility, since most glioma cells express L1. This could be due to the activation of Src pathway and the MAP kinase pathway via p38 [94][95][96][97].

The FGFR-L1 interaction blocking CHD peptide did not have any effect on glioma cell proliferation when the cells were subconfluent. But, there was a reduction of 43% in the % S phase of confluent U-118/L1LE cells incubated with the peptide. Since T98G cells attains G_0 phase at their confluent state, the effect of the peptide cannot be determined. This would likely be due to the different mechanism or receptor activation that controls the rate of proliferation of glioma cells which is dependent on its confluency. This observation has not been recorded previously in glioma cells. This could mean that the rate of proliferation of glioma cells in a tumor mass, equivalent to its confluent state, might signal through FGFR. But when the cells detach from the tumor and tend to migrate, L1-FGFR interaction might facilitate its

migration rather than proliferation. This hypothesis is supported by studies conducted on various FGF ligands having different effects on FGFR. It has been shown previously that FGF signals for cell proliferation and migration occur through different pathways [113][114]. aFGF has been found to have different activity depending on the confluency of the culture. On subconfluent cultures, it promoted Epithelial to Mesenchymal Transition (EMT) and growth arrest, but in confluent cultures it only stimulated DNA synthesis [113].

A cell migration analysis was performed on T98G cells infected with shL1 and truncated FGFR1. Blocking both L1 and FGFRs completely abrogated cell migration. But when L1-conditioned media was added back onto the cells, migration was partially, but significantly, restored. This could mean that L1CAM stimulates migration not only through FGFR but also some other receptor. Integrins have been shown to be another vital receptor for transmitting signals through L1 activation [24][54]. Since the "double negative" cells (T98G/shL1/ΔFGFR1) did not have their migration rate completely restored, this is also evidence for the contribution of another receptor (i.e. integrins) towards T98G cell migration. This is consistent with our previous findings that integrins are involved with L1-mediated migration of T98G cells [60].

T98G/shL1/ΔFGFR1 cells were grown in 1% serum containing media and after 30 hours it was replaced with 10% serum containing media. After 12 hours of incubation, no cells were found to be alive. While T98G/2605, T98GΔFGFR1, T98GshL1, T98G/plko.1, T98G/shL1/2605, T98G/plko.1/2605 cells were found to be surviving. This effect was observed multiple times (data not shown). This shows that

both L1 and FGFR activity could contribute towards a sustained cell survival signal in T98G cells even though it was not conclusive.

Evidence shows that the up regulation of various growth factors and their receptors are correlated with several neoplasms. EGFR amplification is reported in 30-40% of human glioblastoma [106]. Increased cellularity and vascularity characterized by glioblastoma validates the requirement for an increased expression of growth factor receptors. Even though evidence shows that there is no *gene amplification* of FGFRs, the *overexpression* could be due to a generalized response of many cell types to neoplastic transformation [107]. My study shows that regardless of genetic amplification, a receptor (i.e. FGFR) can play a vital role in controlling cancer cell phenotype. This increased expression level of FGFR1 could maintain the constant proliferative and migratory state of high-grade glioma cells.

Although FGF has been thought to be the vital molecule in glioma cells for activating FGFR [64][108], the role of L1CAM has not been elucidated until now. This study not only shows the significance of L1-FGFR interaction on proliferation, but also on migration. Angiogenesis previously was found to be inhibited in ΔFGFR expressing cells [64]. However, knocking out FGF1, FGF2, or FGF8 did not retard embryonic vascular development even though FGFR was shown to be a vital molecule [109][100][111]. If some of the major canonical ligands of FGFR are not responsible for this process, it could be because of other FGFR ligands such as L1CAM.

CONCLUSION

-L1CAM is extensively expressed in glioma tumor tissues as determined from the datasets from a wide range of clinical samples.

-L1CAM controls the rate of proliferation of glioma cells significantly.

-Induced expression of L1CAM in glioma cells increases their rate of migration.

-FGFR1 is over-expressed in glioma tumor tissues regardless of the the grade.

-FGFR inactivation through a dominant negative strategy retards glioma cell migration.

-FGFR1 inhibitor PD173074 also decreased glioma cell migration .

-FGFR1 contributes significantly towards the rate of proliferation of glioma cells.

-L1-FGFR interaction contributes towards glioma cell migration.

-L1-FGFR blocking does not affect proliferation of glioma cells when they are not confluent.

-Blocking L1-FGFR interaction decreases U-118/L1LE cell proliferation when they are confluent.

-L1 induced migration of glioma cells also occurs through other pathways independent of FGFR activation.

-Attenuation of L1CAM and inactivation of FGFR completely abrogates glioma cell migration.

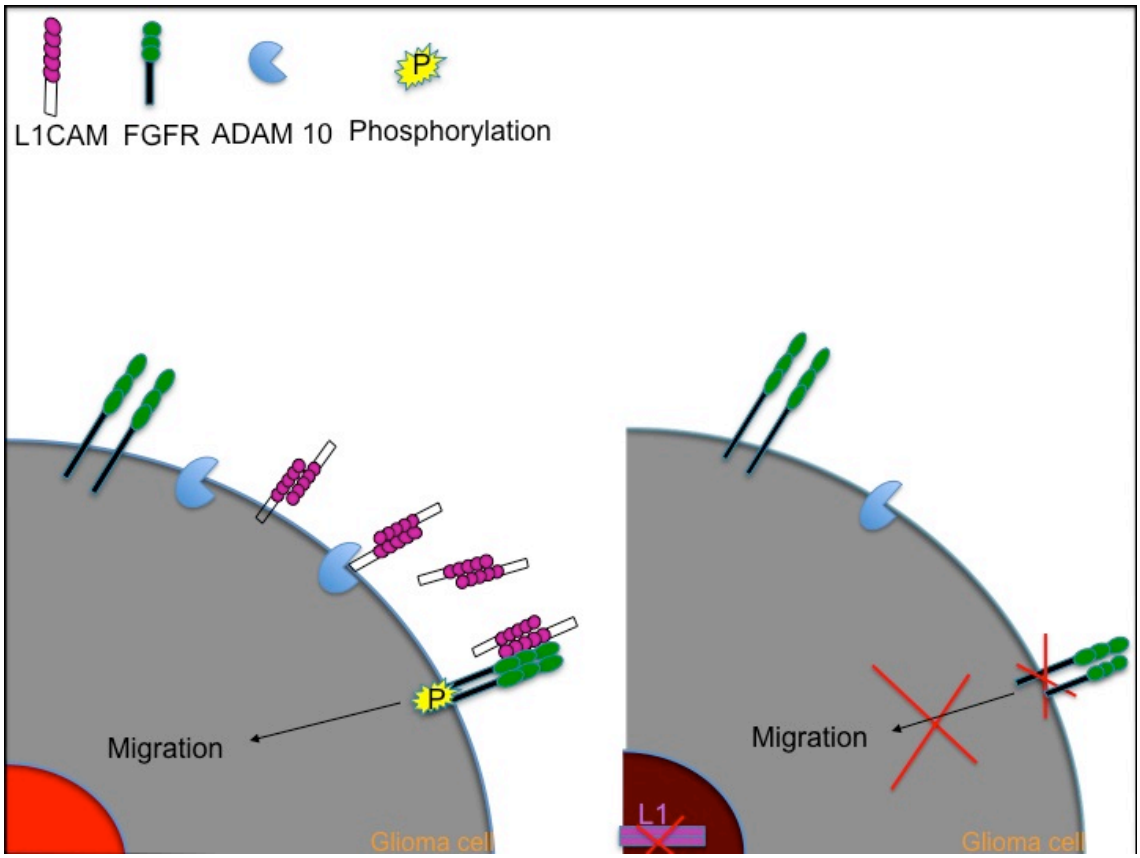

Figure 41 **Model.** An upregulation of cleavage of L1CAM results in binding with FGFR, which translates intercellular signal for migration. While shutting down the expression of L1CAM and inactivating the FGF receptors results in complete termination of migration.

REFERENCES

1. Claes A, Idema AJ, Wesseling P (2007). Diffuse glioma growth: a guerilla war. Acta Neuropathol, 114(5): 443-458.
2. Kleihues, P, F Soylemezoglu, B Schauble, BW Scheithauer, and PC Burger (1995).Histopathology, classification, and grading of gliomas. Glia, 15, 211-221.
3. Wen, P, HA Fine, PM Black, DC Shrieve, E Alexander, and JS Loeffler (1995). High-grade astrocytomas. Neurologic Clinics, 13, 875-900.
4. Almenar Medina S (2009) Anatomía Patológica. Biología Molecular. In: Arribas L, Badal MD, Clavo B et al (eds) Tumores del Sistema Nervioso Central. MPG, Madrid, 49–78.
5. Bao S, Wu Q, Li Z, Sathornsumetee S, Wang H, McLendon RE, Hjelmeland AB, Rich JN (2008). Targeting cancer stem cells through L1CAM suppresses glioma growth. Cancer Res. 68(15):6043-8. PMCID: PMC2739001
6. Houghton J, Morozov A, Smirnova I, Wang TC (2007). Stem cells and cancer. Semin Cancer Biol., 17(3):191-203.
7. Park DM, Rich JN (2009). Biology of glioma cancer stem cells. Mol Cells, 28(1):7-12.
8. Wen PY, Kesari S (2008). Malignant gliomas in adults. N Engl J Med. Jul 31;359(5):492-507.

9. Yuan X, Curtin J, Xiong Y, Liu G, Waschsmann-Hogiu S, Farkas DL, Black KL, Yu JS (2004). Isolation of cancer stem cells from adult glioblastoma multiforme. Oncogene, 23(58):9392-400.
10. Ahluwalia MS, de Groot J, Liu WM, Gladson CL (2010). Targeting SRC in glioblastoma tumors and brain metastases: rationale and preclinical studies, Cancer Lett. 2010 Dec 8;298(2):139-49.
11. Holland EC (2000). Glioblastoma multiforme: the terminator. Proc Natl Acad Sci U S A, Jun 6;97(12):6242-4.
12. Ohgaki H, Kleihues P: Population-based studies on incidence, survival rates, and genetic alterations in astrocytic and oligodendroglial gliomas. *J Neuropathol Exp Neurol* 2005, 64 (6): 479–89.
13. Herron LR, Hill M, Davey F, Gunn-Moore FJ (2009). The intracellular interactions of the L1 family of cell adhesion molecules. Biochem J. 2009 May 1;419(3):519-3.
14. Hortsch M (1996). The L1 family of neural cell adhesion molecules: Old proteins performing new tricks. *Neuron 17*, 587–593.
15. Rathjen, F.G. and Rutishauser, U. (1984). Comparison of two cell surface molecules involved in neural cell adhesion. EMBO J. 3, 461–465
16. Grumet, M., Mauro, V., Burgoon, M.P., Edelman, G.M. and Cunningham, B.A. (1991). Structure of a new nervous system glycoprotein, Nr-CAM, and its relationship to subgroups of neural cell adhesion molecules. J. Cell Biol. 113, 1399–1412.

17. Kamiguchi, H. et al. (1998). The neural cell adhesion molecule L1 interacts with the AP-2 adaptor and is endocytosed via the clathrin-mediated pathway. J. Neurosci. 18, 5311–5321.
18. Brummendorf T, Kenwrick S and Rathjen FG: Neural cell recognition molecule L1; from cell biology to human hereditary brain malformation. *Curr Opin Neurobiol* 1988, 8:87-97.44.
19. Haspel J and Grumet M: The L1CAM extracellular region: a multidomain protein with modular and cooperative binding modes. *Front Biosci* 2003, 8:s1210-s1225. 45.
20. Hortsch M: The L1 family of neural cell adhesion molecules: old proteins performing new tricks. *Neuron* 1996, 17(4):587-593.
21. Kadmon, G. and Altevogt, P. (1997). The cell adhesion molecule L1: species- and cell-type-dependent multiple binding mechanisms. Differentiation 61, 143–150.
22. Kenwrick, S, Watkins A, De Angelis E. (2000). Neural cell recognition molecule L1: relating biological complexity to human disease mutations. Hum. Mol. Genet. 9, 879–886.
23. Weller S, Gärtner J (2001), Genetic and clinical aspects of X-linked hydrocephalus (L1 disease): Mutations in the L1CAM gene. Hum Mutat. 2001;18(1):1-12.
24. Mechtersheimer S, Gutwein P, Agmon-Levin N, Stoeck A, Oleszewski M, Riedle S, Postina R, Fahrenholz F, Fogel M, Lemmon V, Altevogt P (2001). Ectodomain shedding of L1 adhesion molecule promotes cell

migration by autocrine binding to integrins. *Journal of Cell Biology*, 661-674.

25. Thelen K, Kedar V, Panicker AK, Schmid RS, Midkiff BR, Maness PF: The neural cell adhesion molecule L1 potentiates integrin-dependent cell migration to extracellular matrix proteins. *J Neurosci* 2002, 22:4918-4931.
26. Silletti S, Mei F, Sheppard D, Montgomery AM (2000). Plasmin-Sensitive Dibasic Sequences in the Third Fibronectin-like Domain of L1–Cell Adhesion Molecule (Cam) Facilitate Homomultimerization and Concomitant Integrin Recruitment. *Journal of Cell Biology*, 1485-1502.
27. Gavert N, Conacci-Sorrell M, Gast D, Schneider A, Altevogt P, Brabletz T, Ben-Ze'ev A (2005). L1, a novel target of ß-catenin signaling, transforms cells and is expressed at the invasive front of colon cancers. *J Cell Biol*, 168:633–42.
28. Gast D, Riedle S, Issa Y, Pfeifer M, Beckhove P, Sanderson MP, Arlt M, Moldenhauer G, Fogel M, Kruger A, Altevogt P (2008). The cytoplasmic part of L1-CAM controls growth and gene expression in human tumors that is reversed by therapeutic antibodies. *Oncogene.*, 27(9):1281-9.
29. Schmid RS & Maness PF (2008). L1 and NCAM adhesion molecules as signaling coreceptors in neuronal migration and process outgrowth. *Current Opininon in Neurobiology, 18*, 1-6.
30. Hortsch M (2000). Structural and functional evolution of the L1 family: are four adhesion molecules better than one? Mol Cell Neurosci. Jan;15(1):1-10.

31. Malhotra, J.D., Tsiotra.P., Karagogeos, D. and Hortsch, M. (1998). Cis activation of L1-mediated ankyrin recruitment by TAG-1 homophilic cell adhesion. J. Biol.Chem. 273, 33354-33359.
32. Kamiguchi, H. and Lemmon, V. (1997). Neural cell adhesion molecule L1: signaling pathways and growth cone motility. J. Neurosci. Res. 49, 1–8.
33. Kolkova, K., Novitskaya, V., Pedersen, N., Berezin, V. and Bock, E. (2000). Neural cell adhesion molecule-stimulated neurite outgrowth depends on activation of protein kinase C and the Ras-mitogen-activated protein kinase pathway. J. Neurosci. 20, 2238–2246.
34. Loers G, Chen S, Grumet M, Schachner M (2005). Signal transduction pathways implicated in neural recognition molecule L1 triggered neuroprotection and neuritogenesis. J Neurochem. Mar;92(6):1463-76.
35. Boilly B, Vercoutter-Edouart AS, Hondermarck H, Nurcombe V, Le Bourhis X (2000). FGF signals for cell proliferation and migration through different pathways. Cytokine Growth Factor Rev. Dec;11(4):295-302.
36. Asai T, Wanaka A, Kato H, Masana Y, Seo M. 1993. Differential expression of two members of FGF receptor gene family, FGFR‐1 and FGFR‐2 mRNA, in the adult rat central nervous system. Brain Res Mol Brain Res 17: 174-178.
37. Yazaki N, Hosoi Y, Kawabata K, Miyake A, Minami M. 1994. Differential expression patterns of mRNAs for members of the fibroblast

growth factor receptor family, FGFR‐1‐FGFR‐4, in rat brain. J Neurosci Res 37: 445-452.

38. Wang JK, Gao G, Goldfarb M (1994). Fibroblast growth factor receptors have different signaling and mitogenic potentials. Mol Cell Biol;14:181–188.
39. Shaoul E, Reich-Slotky R, Berman B, Ron D (1995). Fibroblast growth factor receptors display both common and distinct signaling pathways. Oncogene;10:1553–1561.
40. Umbhauer M, Penzo-Méndez A, Clavilier L, Boucaut J, Riou J (2000). Signaling specificities of fibroblast growth factor receptors in early Xenopus embryo. J Cell Sci;113:2865–2875.
41. Raffioni S, Thomas D, Foehr ED, Thompson LM, Bradshaw RA (1996). Comparison of the intracellular signaling responses by three chimeric fibroblast growth factor receptors in PC12 cells. Proc Natl Acad Sci USA;96:7178–7183.
42. Hart KC, Robertson SC, Kanemitsu MY, Meyer AN, Tynan JA, Donoghue DJ (2000). Transformation and Stat activation by derivatives of FGFR1, FGFR3, and FGFR4. Oncogene;19:3309–3320.
43. Bellot F, Crumley G, Kaplow JM, Schlessinger J, Jaye M, Dionne CA (1991). Ligand-induced transphosphorylation between different FGF receptors. EMBO J;10:2849–2854.
44. Kimelman, D. & Kirschner, M. Synergistic induction of mesoderm by FGF and TGF-β and the identification of an mRNA coding for FGF in the early Xenopus embryo. Cell 51, 869–877 (1987).

45. De Moerlooze, L. et al. An important role for the IIIb isoform of fibroblast growth factor receptor 2 (FGFR2) in mesenchymal-epithelial signalling during mouse organogenesis. (2000). Development 127, 483–492.
46. Williams EJ, Furness J, Walsh FS, Doherty P. (1994). Activation of the FGF receptor underlies neurite outgrowth stimulated by L1, N-CAM, and N-cadherin. Neuron. 1994 Sep;13(3):583- 94.
47. Doherty, P, Smith, P, and Walsh, FS (1996). Shared cell adhesion molecule (CAM) homology domains point to CAMs signalling via FGF receptors. Perspec. Dev. Neurobiol., 4, 157-168.
48. Klint P, Claesson-Welsh L (1999). Signal transduction by fibroblast growth factor receptors. Front Biosci;4:165-77.
49. Ong SH, Guy GR, Hadari YR, Laks S, Gotoh N. 2000. FRS2 proteins recruit intracellular signaling pathways by binding to diverse targets on fibroblast growth factor and nerve growth factor receptors. Mol Cell Biol 20: 979-989.
50. Mohammadi M, Schlessinger J, Hubbard SR. 1996. Structure of the FGF receptor tyrosine kinase domain reveals a novel autoinhibitory mechanism. Cell 86: 577-587.
51. Kulahin. 2009. Identification of Neural Cell Adhesion Molecule L1-Derived Neuritigenic Ligands of the Fibroblast Growth Factor Receptor.
52. Kiselyov. 2003. Structural Basis for a Direct Interaction between FGFR1 and NCAM and Evidence for a regulatory Role of ATP.

53. Saffell et.al., 1997. Expression of a dominant negative FGF receptor inhibits axonal growth and FGF receptor phosphorylation stimulated by CAMs.
54. Hall H, Walsh FS, Doherty P. (1996). Review: a role for the FGF receptor in the axonal growth response stimulated by cell adhesion molecules? Cell Adhes Commun. Apr;3(6):441-50.
55. Ueno H, Gunn M, Dell K, Tseng A Jr, Williams L. (1992). A truncated form of fibroblast growth factor receptor 1 inhibits signal transduction by multiple types of fibroblast growth factor receptor. J Biol Chem. Jan 25;267(3):1470-6.
56. Suyama K, Shapiro I, Guttman M, Hazan RB. (2002). A signaling pathway leading to metastasis is controlled by N-cadherin and the FGF receptor. Cancer Cell. Oct;2(4):301-14.
57. Gavert N, Ben-Shmuel A, Raveh S, Ben-Ze'ev A (2008). L1-CAM in cancerous tissues. Expert Opin Biol Ther. 2008 Nov;8(11):1749-57.
58. Zecchini S, Bianchi M, Colombo N, Fasani R, Goisis G, Casadio C, Viale G, Liu J, Herlyn M, Godwin AK, Nuciforo PG, Cavallaro U. (2008). The differential role of L1 in ovarian carcinoma and normal ovarian surface epithelium. Cancer Res. Feb 15;68(4):1110-8.
59. Wolterink S, Moldenhauer G, Fogel M, Kiefel H, Pfeifer M, Lüttgau S, Gouveia R, Costa J, Endell J, Moebius U, Altevogt P. (2010). Therapeutic antibodies to human L1CAM: functional characterization and application in a mouse model for ovarian carcinoma. Cancer Res. Mar 15;70(6):2504-15. Epub 2010 Mar 9.

60. Yang M, Li Y, Chilukuri K, Brady OA, Boulos MI, Kappes JC, Galileo DS. (2011). L1 stimulation of human glioma cell motility correlates with FAK activation. J Neurooncol.
61. Valladares A, Hernández NG, Gómez FS, Curiel-Quezada E, Madrigal-Bujaidar E, Vergara MD, Martínez MS, Arenas Aranda DJ. (2006). Genetic expression profiles and chromosomal alterations in sporadic breast cancer in Mexican women. Cancer Genet Cytogenet. 2006 Oct 15;170(2):147-51.
62. Rand V, Huang J, Stockwell T, Ferriera S, Buzko O, Levy S, Busam D, Li K, Edwards JB, Eberhart C, Murphy KM, Tsiamouri A, Beeson K, Simpson AJ, Venter JC, Riggins GJ, Strausberg RL. (2005). Sequence survey of receptor tyrosine kinases reveals mutations in glioblastomas. Proc Natl Acad Sci U S A. 2005 Oct 4;102(40):14344-9. Epub 2005 Sep 26.
63. Loilome W, Joshi AD, ap Rhys CM, Piccirillo S, Vescovi AL, Gallia GL, Riggins GJ. (2009). Glioblastoma cell growth is suppressed by disruption of Fibroblast Growth Factor pathway signaling. J Neurooncol. Sep;94(3):359-66. Epub 2009 Apr 2.
64. Auguste P, Gürsel DB, Lemière S, Reimers D, Cuevas P, Carceller F, Di Santo JP, Bikfalvi A. (2001). Inhibition of fibroblast growth factor/fibroblast growth factor receptor activity in glioma cells impedes tumor growth by both angiogenesis-dependent and -independent mechanisms. Cancer Res. Feb 15;61(4):1717-26.

65. Rousseau B, Larrieu-Lahargue F, Javerzat S, Guilhem-Ducléon F, Beermann F, Bikfalvi A. (2004). The tyrp1-Tag/tyrp1-FGFR1-DN bigenic mouse: a model for selective inhibition of tumor development, angiogenesis, and invasion into the neural tissue by blockade of fibroblast growth factor receptor activity. Cancer Res. 2004 Apr 1;64(7):2490-5.
66. Loilome W, Joshi AD, ap Rhys CM, Piccirillo S, Vescovi AL, Gallia GL, Riggins GJ. (2009). Glioblastoma cell growth is suppressed by disruption of Fibroblast Growth Factor pathway signaling. J Neurooncol. Sep;94(3):359-66. Epub 2009 Apr 2.
67. Sandilands E, Akbarzadeh S, Vecchione A, McEwan DG, Frame MC, Heath JK. (2007). Src kinase modulates the activation, transport and signalling dynamics of fibroblast growth factor receptors. EMBO Rep. 2007 Dec;8(12):1162-9. Epub 2007 Nov 2.
68. Courjal, F. Mapping of DNA amplifications at 15 chromosomal localizations in 1875 breast tumors: definition of phenotypic groups. Cancer Res. 57, 4360–4367 (1997).
69. Jacquemier, J. et al. Expression of the FGFR1 gene in human breast-carcinoma cells. Int. J. Cancer 59, 373–378 (1994).
70. Gorringe, K. L. et al. High-resolution single nucleotide polymorphism array analysis of epithelial ovarian cancer reveals numerous microdeletions and amplifications. Clin. Cancer Res. 13, 4731–4739 (2007).

71. Simon, R. High-throughput tissue microarray analysis of 3p25 (RAF1) and 8p12 (FGFR1) copy number alterations in urinary bladder cancer. Cancer Res. 61, 4514–4519 (2001).
72. Missiaglia, E. Genomic imbalances in rhabdomyosarcoma cell lines affect expression of genes frequently altered in primary tumors: an approach to identify candidate genes involved in tumor development. Genes Chromosom. Cancer 48, 455–467 (2009).
73. Lin, W. M. Modeling genomic diversity and tumor dependency in malignant melanoma. Cancer Res. 68, 664–673 (2008).
74. Xiao, S. FGFR1 is fused with a novel zinc-finger gene, ZNF198, in the t(8;13) leukaemia/lymphoma syndrome. Nature Genet. 18, 84–87 (1998).
75. Roumiantsev, S. et al. Distinct stem cell myeloproliferative/T lymphoma syndromes induced by ZNF198–FGFR1 and BCR–FGFR1 fusion genes from 8p11 translocations. Cancer Cell 5, 287–298 (2004).
76. Kunii, K. FGFR2-amplified gastric cancer cell lines require FGFR2 and Erbb3 signaling for growth and survival. Cancer Res. 68, 2340–2348 (2008).
77. Dutt, A. Drug-sensitive FGFR2 mutations in endometrial carcinoma. Proc. Natl Acad. Sci. USA 105, 8713–8717 (2008).
78. Easton, D. F. Genome-wide association study identifies novel breast cancer susceptibility loci. Nature 447, 1087–1093 (2007). These genome-wide association studies identified an SNP in the second intron of FGFR2 that was associated with an increased incidence of breast cancer.

79. Nord, H. Focal amplifications are associated with high-grade and recurrences in stage Ta bladder carcinoma. Int. J. Cancer 9 Oct 2009 (doi:10.1002/ ijc.24954).
80. Cappellen, D. Frequent activating mutations of FGFR3 in human bladder and cervix carcinomas. Nature Genet. 23, 18–20 (1999). This report describes the detection of somatic FGFR3 mutations in solid tumours that are identical to those underpinning FGFR3-dependent developmental defects.
81. Yagasaki, F. Fusion of ETV6 to fibroblast growth factor receptor 3 in peripheral T-cell lymphoma with a t(4;12)(p16;p13) chromosomal translocation. Cancer Res. 61, 8371–8374 (2001).
82. Bange, J. Cancer progression and tumor cell motility are associated with the FGFR4 Arg(388) allele. Cancer Res. 62, 840–847 (2002).
83. Mohammadi M, Froum S, Hamby JM, Schroeder MC, Panek RL, Lu GH, Eliseenkova AV, Green D, Schlessinger J, Hubbard SR. (1998). Crystal structure of an angiogenesis inhibitor bound to the FGF receptor tyrosine kinase domain. EMBO J. Oct 15;17(20):5896-904.
84. Bansal R, Magge S, Winkler S. (2003). Specific inhibitor of FGF receptor signaling: FGF-2-mediated effects on proliferation, differentiation, and MAPK activation are inhibited by PD173074 in oligodendrocyte-lineage cells. J Neurosci Res. 2003 Nov 15;74(4):486-93.
85. Chen C & Okayama H (1987). High-efficiency transformation of mammalian cells by plasmid DNA. *Mol Cell Biol.*, 7(8): 2745–2752.

86. Fotos JS, Patel VP, Karin NJ, Temburni MK, Koh JT, Galileo DS (2006). Automated time-lapse microscopy and high-resolution tracking of cell migration. *Cytotechnology*, 51, 7-19.
87. Yang M, Adla S, Temburni MK, Patel VP, Lagow EL, Brady OA, Tian J, Boulos MI, Galileo DS. (2009). Stimulation of glioma cell motility by expression, proteolysis, and release of the L1 neural cell recognition molecule. Cancer Cell Int. Oct 29;9:27.
88. Texeira K (2009). Quantitative Analysis Of Breast Cancer Metastasis To The Brain. *Thesis submitted to University of Delaware.*
89. Adla S. (2007). Characterization of the neural cell recognition molecule in breast cancer cells and its role in breast cancer cell motility. Thesis submitted to University of Delaware
90. Beckman M. (2006). CAMs are stopping cancer in its metastatic tracks. J Natl Cancer Inst. 98:576-577.
91. Crossin KL, Krushel LA (2000). Cellular signaling by neural cell adhesion molecules of the immunoglobulin superfamily. Dev Dyn 2000, 218:260-279.
92. Raveh S, Gavert N, Ben-Ze'ev A. (2009). L1 cell adhesion molecule (L1CAM) in invasive tumors. *Cancer Lett.* 282:137-145.
93. DeVore DL, Horwitz HR, Stern MJ. (1995). An FGF receptor signaling pathway is required for the normal cell migrations of the sex myoblasts in C. elegans hermaphrodites. Cell. 83:611±20.
94. La ValleÂ e TM, Prudovsky IA, McMahon GA, Hu X, Maciag T. (1998). Activation of the MAP kinase pathway by FGF-1 correlates with cell

proliferation induction while activation of the Src pathway correlates with migration. J Cell Biol. 141:1647±58.

95. Jaakkola P, Kontusaari S, Kauppi T, Maata A, Jalkanen M. (1998). Wound reepithelialization activates a growth factor-responsive enhancer in migrating keratinocytes. FASEB J. 12:959±69.
96. Cheng H, Cao Y, Olson L. (1996). Spinal cord repair in adult paraple- gic rats: partial restoration of hind limb function. Science. 273:510±3.
97. Tanaka K, Abe M, Sato Y. (1999). Roles of extracellular signal-regu-lated kinase 1/2 and p38 mitogen-activated protein kinase in the signal transduction of basic fibroblast growth factor in endo-thelial cells during angiogenesis. Jpn J Cancer Res. 90:647± 54.
98. Sun L, Hui AM, Su Q, Vortmeyer A, Kotliarov Y, Pastorino S, Passaniti A, Menon J, Walling J, Bailey R, Rosenblum M, Mikkelsen T, Fine HA. (2006). Neuronal and glioma-derived stem cell factor induces angiogenesis within the brain. Cancer Cell. 9(4):287-300.
99. Morrison RS, Yamaguchi F, Bruner JM, Tang M, McKeehan W, Berger MS (1994) Fibroblast growth factor receptor gene expression and immunoreactivity are elevated in human glio- blastoma multiforme. Cancer Res 54:2794–2799.
100. Morrison RS, Yamaguchi F, Saya H, Bruner JM, Yahanda AM, Donehower LA, Berger M (1994) Basic fibroblast growth factor and fibroblast growth factor receptor I are implicated in the growth of human astrocytomas. J Neurooncol 18:207–216. doi: 10.1007/BF01328955

101. Yamada SM, Yamaguchi F, Brown R, Berger MS, Morrison RS (1999) Suppression of glioblastoma cell growth following antisense oligonucleotide-mediated inhibition of fibroblast growth factor receptor expression. Glia 28:66–76.

102. Takahashi JA, Fukumoto M, Kozai Y, Ito N, Oda Y, Kikuchi H, Hatanaka M (1991) Inhibition of cell growth and tumorigenesis of human glioblastoma cells by a neutralizing antibody against human basic fibroblast growth factor. FEBS Lett 288:65–71.

103. Jensen NA, Pedersen KM, Lihme F, Rask L, Nielsen JV, Rasmussen TE, Mitchelmore C (2003) Astroglial c-Myc over- expression predisposes mice to primary malignant gliomas. J Biol Chem 278:8300–8308.

104. Lassman AB, Dai C, Fuller GN, Vickers AJ, Holland EC (2004) Overexpression of c-MYC promotes an undifferentiated pheno- type in cultured astrocytes and allows elevated Ras and Akt signaling to induce gliomas from GFAP-expressing cells in mice. Neuron Glia Biol 1:157–163.

105. Koziczak M, Holbro T, Hynes NE (2004) Blocking of FGFR signaling inhibits breast cancer cell proliferation through down- regulation of D-type cycline.

106. Wong, A. J., Bigner, S. H., Bigner, D. D., Kinzler, K. W., Hamilton, S. R., and Vogelstein, B. Increased expression of the epidermal growth factor receptor gene in malignant gliomas is invariably associated with gene amplification. Proc. Natl. Acad. Sd.USA,84:6899-6903.

107. Yan, G., Fukabori, Y., McBride, G., Nikolaropolous, S., and McKeehan, W. (1993). Exon switching and activation of stromal and embryonic fibroblast growth factor (FGF) FGF receptor genes in prostate epithelial cells accompany stromal independence and malignancy. Mol. Cell Biol., 13: 4513-4522.

108. Yayon, A., Ma, Y. S., Safran, M., Klagsbrun, M., and Halaban, R. (1997). Suppression of autocrine cell proliferation and tumorigenesis of human melanoma cells and fibroblast growth factor transformed fibroblasts by a kinase-deficient FGF receptor 1: evidence for the involvement of Src-family kinases. Oncogene, *14:* 2999–3009.

109. Dono, R., Texido, G., Dussel, R., Ehmke, H., and Zeller, R. (1998). Impaired cerebral cortex development and blood pressure regulation in FGF-2-deficient mice. EMBO J., *17:* 4213–4225.

110. Miller, D. L., Ortega, S., Bashayan, O., Basch, R., and Basilico, C. (2000). Compensation by fibroblast growth factor 1 (FGF1) does not account for the mild phenotypic defects observed in FGF2 null mice. Mol. Cell. Biol., *20:* 2260–2268.

111. Zhou, M., Sutliff, R. L., Paul, R. J., Lorenz, J. N., Hoying, J. B., Haudenschild, C. C., Yin, M., Coffin, J. D., Kong, L., Kranias, E. G., Luo, W., Boivin, G. P., Duffy, J. J., Pawlowski, S. A., and Doetschman, T. (1998). Fibroblast growth factor 2 control of vascular tone. Nat. Med., *4:* 201–207.

112. Lee SH, Schloss DJ, Swain JL. (2000). Maintenance of vascular integrity in the embryo requires signaling through the fibroblast growth factor receptor. J Biol Chem. 275(43):33679-87.

113. Valles AM, Tucker GC, Thiery JP, Boyer B. (1990). Alternative patterns of mitogenesis and cell scattering induced by acidic FGF as a function of cell density in a rat bladder carcinoma cell line. Cell Regul;1:975±88.

114. Richardson TP, Trinkaus-Randall V, Nugent MA. (1999). Regulation of basic fbroblast growth factor binding and activity by cell density and heparan sulfate. J Biol Chem ;274:13534±40.

115. Stein GH (1979) T98G: an anchorage-independent human tumor cell line that exhibits stationary phase G1 arrest in vitro. J Cell Physiol 99(1):43–54

116. Ponte´n J, Macintyre EH (1968) Long term culture of normal and neoplastic human glia. Acta Pathol Microbiol Scand 74(4): 465–486

117. Riedle S, Kiefel H, Gast D, Bondong S, Wolterink S, Gutwein P, Altevogt P (2009) Nuclear translocation and signalling of L1-CAM in human carcinoma cells requires ADAM10 and presenilin/gamma-secretase activity. Biochem J 420: 391–402

118. Yang.M: L1 stimulated glioma cell migration and invasion associates with FAK activation. Ph.D. Dissertation. University of Delaware, Biological Sciences; 2010.

119. Gutmann DH, Hedrick NM, Li J, Nagarajan R, Perry A, Watson MA. (2002). Comparative gene expression profile analysis of

neurofibromatosis 1-associated and sporadic pilocytic astrocytomas Cancer Res; 62(7):2085-91.

120. Li Y, Galileo DS. (2010). Soluble L1CAM promotes breast cancer cell adhesion and migration in vitro, but not invasion. Cancer Cell Int. 15;10:34.

121. Chilukuri K: Role of the released form of L1-CAM in breast cancer cell motility. Masters Thesis. University of Delaware, Biological Sciences; 2010.